

This is an Open Access document downloaded from ORCA, Cardiff University's institutional repository:<https://orca.cardiff.ac.uk/id/eprint/118010/>

This is the author's version of a work that was submitted to / accepted for publication.

Citation for final published version:

Pascual, Justine, Jacobs, Jelle, Sansores-Garcia, Leticia, Natarajan, Malini, Zeitlinger, Julia, Aerts, Stein, Halder, Georg and Hamaratoglu, Fisun 2017. Hippo reprograms the transcriptional response to Ras signaling. *Developmental Cell* 42 (6) , 667-680.e4. 10.1016/j.devcel.2017.08.013

Publishers page: <http://dx.doi.org/10.1016/j.devcel.2017.08.013>

Please note:

Changes made as a result of publishing processes such as copy-editing, formatting and page numbers may not be reflected in this version. For the definitive version of this publication, please refer to the published source. You are advised to consult the publisher's version if you wish to cite this paper.

This version is being made available in accordance with publisher policies. See <http://orca.cf.ac.uk/policies.html> for usage policies. Copyright and moral rights for publications made available in ORCA are retained by the copyright holders.



Hippo reprograms the transcriptional response to Ras signaling

Justine Pascual^{a, #}, Jelle Jacobs^{b, c, #}, Leticia Sansores-Garcia^b, Malini Natarajan^{d, e},
Julia Zeitlinger^{d, f}, Stein Aerts^{c*}, Georg Halder^{b*}, Fisun Hamaratoglu^{a*}

^a Center for Integrative Genomics, University of Lausanne, Lausanne 1015, Switzerland

^b VIB Center for Cancer Biology and KU Leuven Department of Oncology, University of Leuven, Leuven 3000, Belgium

^c Laboratory of Computational Biology, Center for Human Genetics, University of Leuven, Leuven 3000, Belgium

^d Stowers Institute for Medical Research, Kansas City, MO, 64110, USA

^e current address: Department of Molecular Biology, Cell Biology and Biochemistry, Brown University, Providence, RI 02912, USA

^f Department of Pathology and Laboratory Medicine, University of Kansas Medical Center, Kansas City, KS, 66160, USA

[#] Equal contribution

* Correspondence should be addressed to

FH: fisun.hamaratoglu@unil.ch , GH: Georg.Halder@vib.be

and SA: stein.aerts@kuleuven.be

Lead Contact: FH, fisun.hamaratoglu@unil.ch

Abstract

Mutations that lead to hyperactivation of Ras signaling are hallmarks of carcinomas. However, Ras signaling also mediates cell fate decisions and cellular differentiation without causing hyperproliferation during development. It is not known what dictates whether Ras signaling drives differentiation vs. proliferation. Here we show that the Hippo pathway is critical for this decision. Loss of Hippo signaling switches Ras activation from promoting cellular differentiation to aggressive cellular proliferation. Transcriptome analysis combined with genetic tests show that this excessive proliferation depends on the synergistic induction of Ras target genes. Using ChIP-nexus, we find that Hippo signaling keeps Ras target genes in check by directly regulating the expression of two key downstream transcription factors of the Ras pathway: the ETS-domain transcription factor Pointed and the transcriptional repressor Capicua. Our results highlight how independent signaling pathways can impinge on each other at the level of transcription factors, thereby providing a safety mechanism to keep proliferation in check under normal developmental conditions.

Introduction

The development of cancer usually requires the accumulation of multiple genetic aberrations, with most tumors having 2 to 6 driver mutations (Kandoth et al., 2013, Tomasetti et al., 2015). Some of the most frequent driver mutations occur in components of the Epidermal Growth Factor Receptor (EGFR)-Ras-Raf-MAPK pathway, hereafter referred to as the Ras pathway. EGFR is mutated or amplified in nearly one-fifth of all cancers tested, and mutations in the downstream effectors KRAS and BRAF are found in 22.4% and 18.7% of all cancer samples tested, respectively, as tabulated in the Catalogue of Somatic Mutations in Cancer (COSMIC) database (Forbes et al., 2015). These cancer-associated mutations cause hyperactivation of the Ras pathway and have a major contribution to transformation of a normal cell into a cancer cell (Lemmon and Schlessinger, 2010, Burgess, 2008, Vakiani and Solit, 2011). However, hyperactivation of Ras signaling by itself is not sufficient to cause cellular transformation. Thus, activating mutations in the Ras pathway cause only a mild excess in proliferation in different animal models, but can lead to aggressive and metastatic tumors in combination with mutations in other genes such as p53, the cell polarity proteins Scribbled and Discs-large, or components of the JNK and Hedgehog (Hh) signaling pathways (Xia and Land,

2007, Pagliarini and Xu, 2003, Wu et al., 2010, Schnidar et al., 2009, Pearson et al., 2011, Brumby and Richardson, 2003, Chabu et al., 2017, Uhlirova and Bohmann, 2006). However, the underlying mechanisms leading to excess proliferation in response to these combinatorial mutations remain largely unknown. Here, we show that mutations in Hippo signaling strongly synergize with activated Ras signaling and dissect out the underlying mechanism of this synergistic interaction using genomics, genetics and computational approaches. We find that the transcriptional output of Ras signaling is under the tight control of the Hippo pathway. Given that p53, Hh, Scribbled and Discs-large all modulate Hippo signaling (Colombani et al., 2006, Richardson and Portela, 2017, Kagey et al., 2012), our findings also provide a model for how these molecules synergize with Ras during tumorigenesis.

The Hippo pathway is known for its key role in controlling organ growth and progenitor cell proliferation (Hariharan, 2015, Halder and Johnson, 2011, Pan, 2010, Barry and Camargo, 2013). Named after its founding kinase Hippo (Hpo), the pathway coordinately regulates cell proliferation and cell death. Cells that lack Hippo signaling proliferate faster and are resistant to apoptotic stimuli, a combination that leads to dramatic tissue overgrowths in flies and mice. Notably, loss of Hippo signaling in the mouse liver leads to tumor formation (Zhou et al., 2009, Song et al., 2010, Lee et al., 2010, Lu et al., 2010) and YAP, the transcriptional effector of Hippo signaling, is an established oncogene in the ovary, lung, liver and breast (Harvey et al., 2013, Zanconato et al., 2016).

The components and mechanisms of Hippo signaling are highly conserved in animals. At the core of the Hippo pathway is a kinase cascade where in *Drosophila* the Hpo kinase (Mst1/2 in mammals) phosphorylates and activates the Warts kinase (Wts, Lats1/2 in mammals). The main substrate of activated Wts/Lats is the transcriptional co-activator Yorkie (Yki, YAP/TAZ in mammals), which is retained in the cytoplasm upon phosphorylation. In the absence of Hpo pathway activity, Yki translocates into the nucleus and binds to the TEAD family transcription factor Scalloped (Sd, TEAD1-4 in mammals) and other transcription factors. By default, Sd is a repressor, but the binding of Yki converts Sd into an activator and together they then drive the expression of pro-survival and proliferation genes, such as *cyclin E*, *diap-1* and *bantam* microRNA (Koontz et al., 2013, Hariharan, 2015). Multiple upstream regulators including the FERM domain proteins Merlin (Mer) and Expanded (Ex), the atypical cadherins Fat and Dachous, cell polarity and mechanical forces

have been shown to activate the Hpo kinase (Grusche et al., 2010, Piccolo et al., 2014, Legoff et al., 2013, Mao et al., 2013, Karaman and Halder, 2017).

Here, we studied the effects of combining mutations in the Ras and Hippo pathways. Notably, reducing Hippo signaling in cells harboring activating mutations in the Ras pathway caused strongly synergistic overgrowth in *Drosophila* imaginal discs. We find that in such discs, the differentiation program is shut down. We investigated the molecular basis of this synergy using genomics and show that the Hippo pathway acts as a gatekeeper for Ras signaling output by restricting the expression levels of its transcriptional targets. This is achieved *via* direct transcriptional control of the transcription factors of the Ras pathway. In *Drosophila*, MAPK regulates gene expression via modulating the protein stability of three transcription factors: the repressor Capicua (Cic) and the ETS domain proteins Pointed (Pnt) and Yan (Shilo, 2014, Jiménez et al., 2012). We show that Cic and Pnt are direct Yki/Sd targets. Thus, in healthy cells, Hippo signaling acts as a break that restrains the tumorigenic potential of activating mutations in the Ras pathway. Inactivating mutations in the Hippo pathway, however, unmask this potential and synergistically promote hyperproliferation and tumor development.

Results

Simultaneous deregulation of Ras and Hippo signaling induces synergistic overgrowth

To study the effects of combinatorial mutations in the Ras and Hippo pathways, we simultaneously activated Ras signaling and repressed the Hippo pathway in *Drosophila* imaginal discs, simple epithelial structures that are widely used to investigate mechanisms of growth control and tissue patterning. To activate Ras signaling, we expressed constitutively active oncogenic versions of EGFR (EGFR^{top}), Ras (Ras^{V12}), or Raf (Raf^{GOF}) (Queenan et al., 1997, Scholz et al., 1997, Stemerink and Jacobs, 1997, Brand and Perrimon, 1994). To deregulate Hippo signaling, we used animals that were homozygous for null mutations in the Hippo pathway component *expanded* (*ex*) (Hamaratoglu et al., 2006). Loss of *ex* does not fully abolish Hippo pathway activity and *ex* mutant wing discs showed mild overgrowth characteristic for hypomorphic Hippo loss-of-function phenotypes (Fig.1A-B). Similarly, overexpression of activated EGFR in a central stripe in wing discs using the *dpp-Gal4* driver only caused a widening of the expression domain marked by GFP co-expression (Fig.1C). Strikingly, however, expressing activated EGFR in *ex* mutants caused massive overgrowth of mutant wing discs (Fig.1D-D'). Double

mutant larvae pupated up to two days later than controls when discs continued to grow and eventually folded onto themselves. Such cooperative over-proliferation in response to EGFR/Ras activation was formerly described in cells that harbor mutations in the Hippo pathway components *fat* (Garoia et al., 2005) and *wts* (Pagliarini and Xu, 2003). Notably, expression of activated Ras or Raf in *ex* mutants caused the same dramatic overgrowth phenotypes (Fig.S1A). Furthermore, the enormous overgrowths in the presence of EGFR^{top} and *ex* mutants was evident in multiple tissues including eye, antenna, wing, leg, and haltere imaginal discs (Fig.1E-H and not shown). Therefore, activated Ras signaling synergistically interacts with deregulated Hippo signaling to drive tissue overgrowth and this interaction is independent of the type of imaginal discs.

The synergy between Ras and Hippo signaling occurs via the downstream effectors Cic and Yki

We next investigated at which level of the signal transduction cascades the synergy operates. First, we overexpressed EGFR together with Yki, the downstream transcriptional co-activator of the Hippo pathway. Again this caused highly synergistic overgrowth phenotypes (Fig.S1A), indicating that the synergy operates at the level of the downstream transcription effector of the Hippo pathway.

To determine the level of interaction in the Ras pathway, we next tested mutations in the Cic transcription factor. Cic is a HMG domain transcriptional repressor that mediates the effect of Ras on cell proliferation during imaginal eye disc development (Tseng et al., 2007). Cic is a suppressor of cell proliferation in imaginal discs and activated MAPK phosphorylates Cic, causing its degradation. Ras signaling is required for cell proliferation and cell type specification. Thus, cells with a complete loss of Ras signaling, due to mutations in *egfr*, *ras*, or *raf*, do not proliferate and fail to differentiate (Fig.2B) (Yang and Baker, 2001, Yang and Baker, 2003). The failure of *ras* mutant cells to proliferate is due to ectopic Cic activity because *ras*, *cic* double mutant cells proliferate normally (Fig.2C) (Tseng et al., 2007). Despite the strong rescue in cell proliferation, removal of Cic does not rescue the photoreceptor specification defects of *ras* mutant cells. Double mutant cells contribute to the adult eye, but cannot differentiate into photoreceptor cells (Fig.2C). Therefore, Cic is a major effector of Ras signaling in proliferation control (Tseng et al., 2007).

We then analyzed the interaction between loss of Cic and loss of Hippo signaling. While deletion of *cic* alone increased cell proliferation in eye discs only slightly, if at

all (Fig.2A), simultaneous deletion of *cic* together with *wts* enhanced the *wts* mutant phenotype and triggered massive overgrowth beyond the *wts* phenotype (Fig.2D-E). As previously observed, *wts* mutant cells occupied the majority of the tissue and led to overgrown organs (Justice et al., 1995, Xu et al., 1995), and a few animals made it into adults (Fig.2D). However, no adults with *cic wts* clones were recovered (Fig.2E).

We then induced clones with the pan-eye and wing disc drivers *ey-FLP* and *ubx-FLP* in combination with the *Minute* technique to produce imaginal discs that were nearly entirely mutant (Fig.3) (Morata and Ripoll, 1975). Eye and wing discs with *cic wts* double mutant clones had dramatic overgrowth phenotypes that caused the discs to fold onto themselves (Fig.3A-D). Time course analysis and quantifications showed that animals with *cic wts* double mutant wing discs had extended larval periods by about four days similar to animals with *wts* mutant discs. Mutant cells continued to proliferate during this extra time, and *cic wts* double mutant discs were consistently larger than *wts* discs reaching up to 10 times the normal disc size (Fig.3E-F). Importantly, ectopic Yki also synergized with Cic knock-down in causing tissue expansion (Fig.S1B-C). Hence, deregulating the Ras and Hippo pathways at the level of their downstream transcription factors produced the same highly synergistic overgrowths. Altogether, these data show that the synergy between the Hippo and Ras pathways is at the level of transcription.

Loss of Wts and Cic synergistically activates Ras target genes

Because the synergy between the Ras and Hippo pathways is at the level of the downstream transcription factors, the two pathways may converge on a set of synergistically regulated target genes that are activated only when both pathways are deregulated. We therefore performed genome-wide expression analyses (RNA-seq) in control, *cic* and *wts* single mutant, as well as *cic wts* double mutant wing discs to identify synergistically regulated target genes.

Mutations in *wts* cause developmental delay and we thus produced gene expression profiles by RNA-seq at day 5 in all genotypes and at day 9 in *wts* single mutant and *cic wts* double mutant wing discs generated using *ubx-FLP* and a Minute chromosome (as shown on Fig.3E). We focused on genes with a minimum average expression of 50 counts across all samples and significant upregulation was defined as a minimum 1.4-fold increase, with less than 1% false discovery rate (log FC > 0.5 and adjusted P-value < 0.01). We found that the expression of 350 genes was significantly upregulated in day 5 *cic wts* double mutant wing discs compared to discs

with wild-type control clones. Importantly, cell polarity was intact in the day 5 *cic wts* discs (not shown) and hence the transcriptional changes we see at this stage are not a consequence of polarity loss. We then classified these genes into four different groups, based on day 5 expression levels, using SOTA (self-organizing tree algorithm), an unsupervised clustering method (Herrero et al., 2001, Dopazo and Carazo, 1997). The first and largest group comprised 295 genes (84% of differentially expressed genes) that were up-regulated in *wts* single and *cic wts* double mutant discs, but not affected in *cic* mutants (Fig.4A). The upregulation of these genes was thus mostly attributed to the *wts* mutation and we refer to this group as the “Wts cluster”. Notably, this cluster contained the known Yki targets *kibra*, *ex*, *wts*, *dm* (a.k.a. *Myc*) and *llp8* (a.k.a. *Dilp8*) (Pan, 2007, Boone et al., 2016, Neto-Silva et al., 2010, Park et al., 2016, Ziosi et al., 2010), validating the gene expression data (Fig.4B). CycE and DIAP1 were also induced in *wts* and *cic wts* mutant discs but their fold increase was below our cutoff with logFC values of 0.37 and 0.35 respectively (Fig.4B). The second and smallest cluster contained only 12 genes, which were upregulated in *cic* and in *cic wts* mutant discs, but were not significantly influenced by loss of *wts*, hence we named it the “Cic cluster” (Fig.4C). The genes in this cluster were mostly uncharacterized and non-conserved genes. The third “additive” cluster had 17 genes that were mildly upregulated in *wts* and *cic* single mutants and showed additive upregulation in the double mutant (Fig.4D). These genes are potentially shared target genes of Yki and Cic and included *sdr* (*secreted decoy of InR*), a modulator of insulin signaling (Okamoto et al., 2013); *shifted* (*shf*), a modulator of Hh signaling (Glise et al., 2005, Gorfinkiel et al., 2005); and the ribosomal protein RpL38 (Marygold et al., 2005).

The most interesting fourth cluster had 26 genes that were strongly induced in *cic wts* double mutants but were largely unaffected in *cic* and *wts* single mutants; hence we coined this set the “synergistic cluster” (Fig.4E). In addition to these genes, closer inspection of the *wts* cluster revealed that 28 of the 295 genes were more than 1.3 fold higher in the *cic wts* double mutants compared to *wts* alone although they were not induced or even down-regulated in *cic* clones. These genes were thus also synergistically regulated by Cic and Wts and were reclassified into the synergistic group (Fig.4F).

Surprisingly, the most striking feature of the synergistic genes was a strong signature of Ras pathway target genes. Synergistically upregulated Ras target genes included *argos* (*aos*), which encodes a secreted antagonist of Ras signaling (Golembo et al.,

1996, Schweitzer et al., 1995); *sprouty (sty)*, an intracellular inhibitor of Ras signaling (Caschi et al., 1999); and *Nf1*, a negative regulator of Ras activity (Ballester et al., 1990, Martin et al., 1990, Xu et al., 1990, Buchberg et al., 1990). These genes are feedback regulators of Ras signaling in multiple tissues and cell types. Most prominently, the major transcriptional activator of the pathway *pointed (pnt)* (Shilo, 2014) was also synergistically induced in the double mutants. These data thus show that Ras signaling output is strongly upregulated in *cic wts* double mutant cells, much above the levels detected in *cic* or *wts* mutant cells. Therefore, simultaneous loss of *cic* and *wts* resulted in a synergistic hyperactivation of Ras output.

The discovery of 54 genes that were synergistically upregulated in response to concomitant loss of *wts* and *cic* reveals that the synergistic overgrowth phenotype of the double mutant is not a trivial consequence of simultaneous deregulation of two unconnected growth control pathways. Rather, the existence of this synergistic gene set shows that activation of one or the other pathway is not sufficient to upregulate their expression and thus that Cic and Wts act as dominant inhibitors on their expression. The discovery of this synergistically deregulated gene set then prompted two questions: First, what are the transcription factors that regulate the synergistically regulated genes? And second, how does the deregulation of the Hippo pathway induce their expression?

iRegulon identifies three key transcription factors that mediate the synergy

To understand the mechanisms that regulate the transcription of the synergistic genes and to elucidate how Ras target genes were hyper-induced in double mutant cells, we searched for transcription factor binding sites that were enriched near the genes of the four gene clusters using iRegulon, a sequence-based motif discovery tool (Janky et al., 2014). iRegulon reverse-engineers a gene regulatory network from the expression data by identifying enriched motifs for transcription factors in a given set of genes (Janky et al., 2014). We focused our search on the introns and 5kb upstream region of each gene. Reassuringly, one of the top motifs (normalized enrichment score (NES) of 4.3, see Methods) in the Wts cluster belonged to the Sd transcription factor, and high confidence Sd binding sites were detected in 123 of 295 genes in this cluster and in all known direct Sd target genes (Atkins et al., 2016). The very top motif, however, belonged to the AP-1 transcription factors (NES=4.76), found enriched near 154 genes, indicating the involvement of JNK signaling. Notably, the AP-1 transcription factors, *Atf3* and *Pdp1*, are themselves part of the Wts cluster,

suggesting that JNK activation is a downstream effect of Yki activity consistent with the recent literature (Ma et al., 2015).

Surprisingly, the Cic cluster was not enriched for Cic binding sites, as only one gene, CG32354, had a Cic motif. However, iRegulon analysis on the synergistically induced genes (Fig.S2A) identified the Cic binding motif as the top hit with very high confidence (NES=6.3), followed by Stat92E (NES=4.3) and Pnt (NES=3.4) motifs (Fig.5A). Indeed, the previously identified Cic target genes *pnt* and *aos* (Roch et al., 2002, Jin et al., 2015) were in this synergistic cluster. Therefore, we embarked on to determine whether other synergistically regulated genes are also direct Cic targets.

Cic directly regulates synergistically induced genes

We defined Cic target genes genome-wide using ChIP-nexus (chromatin immunoprecipitation experiments with nucleotide resolution through exonuclease, unique barcode and single ligation), a robust ChIP-exo protocol that allows high resolution mapping of binding sites (He et al., 2015). We used the Cic signal in *cic wts* mutant discs as background. Combining the ChIP-nexus signal with motif enrichment to determine high confidence Cic peaks, we identified over 100 regions bound by Cic. We then further selected those peaks that were near genes that are induced in *cic wts* discs compared to wild-type. These strict criteria gave us a list of 19 high-confidence Cic target genes (Fig.S2B). Strikingly, this set contained many regulators of the Ras pathway: the Spitz (Spi) ligand, and the negative feedback regulators Aos, Sty, Nf1, and Sulfated (Sulf1) (Butchar et al., 2012). Hence, Cic is a key factor for feedback regulation of Ras signaling.

Next, we asked which factors might regulate the expression of these 19 Cic target genes using iRegulon. As expected, iRegulon identified the Cic motif as the top hit (NES=7.3). In addition, regulatory regions of Cic target genes were also enriched for Pnt (NES=4.5) and Stat92E (NES=4.4) binding motifs (Fig.5B), similar to the predictions for synergistically induced genes. Indeed, seven of the 19 Cic target genes were part of the synergistically induced gene set. These were the two known Cic targets *pnt* and *aos*; three other Ras pathway genes *sty*, *nf1* and *sulf1*; Leucine-rich tendon-specific protein (Lrt) and Brinker (Brk), the transcriptional repressor of Dpp signaling. Therefore, induction of genes that are normally repressed by Cic is the main feature of our synergistic network and at least seven of our synergistic target genes are direct Cic targets.

The finding that synergistically regulated genes are highly enriched for Cic target genes is striking as it shows that the repressor function of Cic on its target genes is dependent on the level of Yki activity. Thus, while Cic represses the expression of Ras target genes, loss of this brake needs to be combined with activation of Yki-Sd to strongly induce their expression. This then prompted the question whether the Yki-Sd complex directly regulates Cic target genes.

Sd and Cic do not compete for DNA binding

Intriguingly, the consensus DNA-binding sequences of Sd (CATTCC) and Cic (CATT(C/G)A) are very similar and differ only at one position. Hence, Sd may directly compete with Cic for binding to regulatory sequences. We tested this hypothesis using the ChIP-nexus data for Cic and also performed ChIP-nexus for Sd. Combining ChIP-nexus signal with motif enrichment identified 800 regions bound by Sd in the genome of wing disc cells. Strikingly, we did not find binding sites that were bound by both Sd and Cic in wild-type wing discs. We then compared Sd binding between *wts* and *cic wts* mutant discs to ask whether Sd now occupies more sites. However, we did not detect new Sd peaks where Cic normally binds. Therefore, Sd does not regulate Cic target genes by competing with Cic for binding the DNA.

We also tested whether Cic can regulate Sd target genes, by searching for Cic peaks in their regulatory regions. We did not find any Cic binding in the prominent Yki-Sd target genes *DIAP1*, *ex*, *wts*, *ft*, *ds*, *fj* or *ilp8*. On the other hand, these regulatory regions were enriched for Sd motifs and had Sd binding as expected. In agreement with these findings, the expression of Yki-Sd target genes were induced at comparable levels in *wts* and in *cic wts* mutant discs (Fig.4B), supporting the conclusion that Cic does not regulate the expression of Yki target genes. Therefore, we conclude that Sd and Cic do not affect each other's ability to bind to target DNA in vivo and their binding motifs, despite only a single nucleotide difference, are clearly distinct.

JAK-STAT signaling and Pnt contribute to the synergistic overgrowth

iRegulon found no enrichment for Sd binding sites within our synergistic gene set. However, in addition to the Cic motif, this gene set was enriched for Pnt and Stat92E binding sites. Stat92E is the transcription factor of the JAK-STAT pathway, another important pathway in tumorigenesis (Amoyel et al., 2014, Zoranovic et al., 2013). 21 of our 46 synergistic genes, including Pnt itself, are predicted to be regulated by Pnt, Cic and Stat92E together (Fig.5A). More than half of our synergistic genes (27/46)

had binding sites for at least 2 out of these 3 factors (Fig.5A). Therefore, we tested the importance of Pnt and Stat92E for the synergistic overgrowth.

First, we found that the ligands of the JAK-STAT pathway, the Unpaired cytokines Upd1 (a.k.a. os), Upd2 and Upd3 are highly upregulated (2.1; 2.6; 2.4 fold respectively) in day 5 *wts* mutant discs (Fig.5C). Upd levels stayed high at day 9 *wts* discs and were further upregulated in *cic wts* double mutant discs (3; 6.18; 4.5 fold, respectively) (Fig.5C). Hence, having upregulated Upd ligand expression, JAK-STAT signaling is likely more active in *wts* and *cic wts* mutant cells. JAK-STAT signaling is frequently implicated in human cancer and it is commonly induced in *Drosophila* tumor models (Atkins et al., 2016, Davie et al., 2015, Wu et al., 2010). We then tested whether JAK-STAT activation is important for the synergistic overgrowth of *cic wts* mutants by expressing an inhibitor of the pathway, Socs36E (Stec et al., 2013), in our synergistic background (activated EGFR expression in *ex* background). Co-expression of Socs36E efficiently suppressed the overgrowth phenotype in both wing and eye discs (Fig.5F-G vs 5D-E). Notably, the expression of the Upd genes is regulated by the Yki-Sd complex (Bunker et al., 2015) and we found ChIP-nexus peaks and corresponding motifs for both Sd and Cic near the *upd* genes (Fig.S2C). Altogether, these results show that the transcriptional regulation of the Upd genes and the activation of JAK-STAT signaling is an important contributor to the synergy between the Hippo and Ras pathways.

We then used the same assay to test the contribution of Pnt upregulation to the synergistic phenotype. We constructed a stock where *pnt-RNAi* is under the control of the *dpp-Gal4* driver. These flies are viable, fertile and only have mild venation defects on their wings (not shown), suggesting that Pnt function is only slightly reduced but largely intact in this background. However, this mild downregulation of Pnt activity was sufficient to prevent the development of full-fledged synergistic overgrowth. Discs that expressed *pnt-RNAi* in addition to activated EGFR in an *ex* mutant background did not display the full-grown synergistic overgrowth phenotype (Fig.5H-J). Therefore, high Pnt levels are important for the synergistic overgrowth obtained when both Ras and the Hippo pathways are manipulated.

Yki-Sd controls the expression of the Ras pathway transcription factors Pointed and Capicua

Having established that the network predicted by iRegulon is indeed driving the synergistic growth, and that Yki-Sd can influence this network via induction of Upd

transcription, we asked whether Yki-Sd could also regulate the other nodes of the network: Pnt and Cic.

We first had a closer look at the regulation of Pnt. The PntP2 isoform is known to be activated by MAPK phosphorylation and drives the expression of PntP1 in eye discs (Shwartz et al., 2013). In addition, Cic negatively regulates Pnt expression in intestinal stem cells (Jin et al., 2015). To characterize its potential regulation by Hippo signaling, we generated antibodies against Pnt, which detected a pattern identical to dpERK and complementary to Cic in the wing and eye discs (Fig.6A-B and S3A-B). Removal of Cic was sufficient to derepress Pnt expression in wild-type and *ex* mutant cells (Fig.6C-C' and S3F-F'). Since *cic wts* mutant clones occupy large areas, Pnt was expressed widely and lost all pattern in *cic wts* discs (Fig.S3G-G'). These data confirm a tight regulation of Pnt expression by Ras signaling and establish Cic as an important regulator of *pnt* expression in imaginal discs. Direct regulation of Pnt by Cic is also strongly supported by our ChIP data. Of the 100 top Cic peaks in the genome of wing disc cells, 7 were in the *pnt* region and corresponded to Cic motifs (Fig.6D, Cic ChIP signal is shown in red; Sd ChIP signal is shown in blue). Furthermore, the RNA-seq data shows that transcription of *pnt* is induced when the repressor Cic is removed (Fig.5C). Notably, RNA levels of *pnt* are further increased in *cic wts* double mutant discs, although there is no increase in *wts* single mutants (Fig.5C). In fact, *pnt* is expressed at lower levels in *wts* and *ex* mutant discs (Fig.5C and S3E), probably due to higher Cic levels. Therefore, there must be another, positive input into *pnt* expression that depends on Yki-Sd (Fig.5A). Indeed, our ChIP-nexus detected a strong Sd peak containing a Sd motif (blue) in the *pnt* gene, which is also enriched for Pnt (green) and Stat92E (purple) binding sites (Fig.6D). We conclude that Cic, Yki-Sd, Stat92E, and Pnt itself control *pnt* transcription, and that repression by Cic is dominant over the activating inputs.

Finally, we investigated whether Cic is a Sd target gene. We found multiple Sd ChIP-nexus peaks with corresponding Sd binding motifs in the *cic* gene region (Fig.6F). However, *cic* RNA levels, as well as Cic protein levels, were only slightly higher in *wts* mutant wing discs (Fig.5C, 1.1 fold in day 5 and 1.23 fold in day 9 discs). On the other hand, Cic accumulation was obvious in eye discs posterior to the morphogenetic furrow and in-between the clusters of differentiating photoreceptor cells (Fig.6E-E''), where Cic is normally present at low levels (Fig.S3B). Cic is expressed at high levels and uniformly in the wing discs, except for the cells where MAPK leads to its degradation (Fig.6A). We thus hypothesized that Yki-Sd are

required for the high uniform Cic expression. Indeed, knockdown of Yki in the posterior half of wing discs reduced Cic levels (Fig.6G-H'). Hence, induction of Cic transcription by Yki-Sd increases the threshold of Ras activity that is required to induce its target genes.

Discussion

The main conclusion from our study is that Hippo activity determines the outcome of Ras signaling. In our model, combined action of Hippo signaling and the repressor Cic prevents excessive proliferation and allows differentiation by keeping a set of key target genes off (Fig.7). Cic suppresses many of these genes directly and Hippo signaling prevents their full activation at least partially by keeping both JAK/STAT activity and Pnt levels low. This model is based on three key observations. First, we found that activated Ras signaling has different outcomes in wild-type discs vs *ex* mutant discs. While hyperactivation of Ras signaling in a wild-type disc promotes cellular differentiation, Ras activation combined with loss of *ex* drives aggressive hyperproliferation. Second, we defined a set of synergistic genes that were strongly induced only when the repressor Cic was removed and Yki was simultaneously activated. These genes were predicted to be regulated by Cic, Pnt, and Stat92E. Indeed, we confirmed that high Pnt levels and JAK/STAT activity contributed to the synergistic overgrowth phenotype. Lastly, we found that the Hippo pathway transcription factor Sd directly regulates the expression of the JAK/STAT ligands and the Ras signaling transcription factors Cic and Pnt. When Hippo signaling and Cic are simultaneously inhibited, the synergistic genes and the Yki targets are expressed at high levels, paving the way to cellular transformation.

We defined a small set of direct Cic target genes in wing discs. Identification of many feedback regulators of Ras signaling among direct Cic targets emphasizes the central role of this protein in controlling Ras output despite the weak phenotypic consequences of its removal. Notably, Cic expression is complementary to that of the other two transcription factors of Ras signaling, Pnt and Yan (Fig.S3A-C). Indeed, Cic controls Pnt transcription in multiple tissues, but our RNA-seq and ChIP-nexus data on wing discs suggests Cic does not regulate Yan.

Our data reveal a fundamental interaction between the Ras and Hippo pathways occurring at the level of their downstream transcription factors. Other points of crosstalk have been reported in the literature. Most prominently, MAPK was suggested to phosphorylate and activate the LIM domain protein Ajuba, a negative

regulator of the Wts kinase (Reddy and Irvine, 2013). Similarly, oncogenic Ras can induce Yap activation (Reddy and Irvine, 2013, Hong et al., 2014). We confirmed that overexpression of constitutively active EGFR or Ras induced the expression of the Yki regulated reporter gene *ex-lacZ* (Fig.S4A-B). Surprisingly however, this was not a general effect and was dependent on the position of the clone. Thus the effect of Ras hyperactivation on the Hippo pathway depends on the fate of a cell. Likewise, only a fraction of patients with activating mutations in Ras have elevated YAP levels paralleling the context dependency that we observed in discs (Lin et al., 2015). Unlike activation of Ras, loss of *cic* did not induce Yki activity. Notably, this was true in a wild-type background and in *ex* and *wts* mutant backgrounds in which loss of *cic* caused synergistic overgrowth (Fig.S4C-F). Two conclusions follow from these results. First, Ras signaling crosses over to the Hippo pathway only upstream of Cic, consistent with the model that MAPK regulates the activity of Ajuba (Reddy and Irvine, 2013). Second, the synergy between Ras and Hippo signaling cannot depend on the regulation of Hippo pathway activity by Ras signaling because loss of *cic* synergized with loss of *wts* in growth control even though Cic does not affect Yki activity. Thus, the synergy between the Hippo and Ras pathways is not due to a general activation of Yki in response to loss of Cic. Rather, we show that the synergy is due to hyperactivation of the Ras signaling output, which is under direct Yki-Sd control. Therefore, there are at least two points of crosstalk between the two pathways: one upstream of Cic via Ajuba and another at the level of transcription factors as described here.

Strikingly, in the *cic wts* double mutant discs, the activities of the other major developmental pathways are reduced: Dpp, Hh, N and Wg signaling activity readouts are expressed at low levels, suggesting a block in the differentiation program (Fig.S5A). Activation of two key Cic target genes, Sulf1 and Brk, are likely to account for this observation. Sulf1 encodes an extracellular protein from the endosulfatase family that regulates the amount and pattern of sulfate groups on heparan sulfate proteoglycans (HSPGs). HSPGs in turn play major roles on morphogen distribution and patterning (Yan and Lin, 2009). Accordingly, Sulf1 was linked to dampening the activity of Wg and Hh signaling pathways (Kleinschmit et al., 2013, You et al., 2011, Wojcinski et al., 2011). Brk, the default repressor of Dpp signaling (Affolter and Basler, 2007), is also a direct Cic target and is highly induced in *cic wts* cells. As a result of the action of Sulf1, Brk and potentially others, we see a block in differentiation signature in *cic wts* double mutant cells (Fig.S5A). In these cells, the readout for Ras signaling is highly upregulated, and simultaneously Dpp, N, Wg and

Hh pathways are downregulated. Consequently, *cic wts* cells lose their differentiation potential and proliferate aggressively (Fig.S5B). Therefore, combined mutations in Hippo and Ras pathways are especially dangerous as both breaks that dampen the transformation potential of a cell are removed (Fig.7). We show that Cic and its targets are central to Ras driven tumorigenesis and the choice between differentiation vs proliferation. Activation of Yki/YAP along with Cic degradation switches the response of a cell from differentiation to proliferation by allowing full activation of Cic targets.

Our analysis of the mechanism by which Hippo and Ras synergise to produce massive tissue overproliferation in flies is likely to be relevant to tumour formation in vertebrates. Recent work indicates that if activation of Ras or Raf is coupled with amplification of the YAP region, the resulting carcinomas are more aggressive and resistant to MEK and Raf inhibitors (Lin et al., 2015). It has also been shown that mutations in Nf2, an upstream regulator of Hippo, cooperate with activating Ras mutations in a mouse model of thyroid cancer and that co-expression of Ras and YAP lead to brain tumor formation in zebrafish (Garcia-Rendueles et al., 2015, Mayrhofer et al., 2017). These findings bring forth the conservation of tumor suppressor pathway structures and underline the need for a mechanistic understanding such as the one exposed here. Our results argue that the transcriptional output of Ras signaling is under Hippo control and that Cic targets can only be fully activated when Yki/YAP is active (Fig.7). Requiring Yki activation and simultaneous removal of Cic for full induction, such “synergy genes” may represent attractive drug targets.

Acknowledgements:

Library preparation and RNA sequencing were done by Lausanne Genomic Technologies Facility. Confocal imaging was done at the Cellular Imaging Facility of University of Lausanne. We thank Mardelle Atkins for advice on RNA-seq sample preparation and Cynthia Staber for antibody design. We are grateful to Jeffrey Johnston for initial processing of the raw ChIP data and Wanqing Shao for help with GEO submission of the ChIP-nexus data. We thank Vincent Dion, Richard Benton and members of the Hamaratoglu Lab for suggestions on the manuscript.

We thank Martin Müller (Affolter Lab, Biozentrum), Iswar Hariharan (UC Berkeley), Graeme Mardon (Baylor College of Medicine), Benny Shilo (Weizmann Institute), Jordi Casanova (IRB Barcelona) and Robert Holmgren (Northwestern University) for

fly stocks and antibodies. The anti-Elav (7E8A10) and anti-Yan (8B12H9) antibodies developed by Gerald Rubin were obtained from the Developmental Studies Hybridoma Bank, created by the NICHD of the NIH and maintained at The University of Iowa, Department of Biology, Iowa City, IA 52242. Stocks obtained from the Bloomington *Drosophila* Stock Center (NIH P40OD018537) and Vienna Drosophila Resource Center (VDRC, www.vdrc.at) were used in this study.

Funding: This work is funded by a Swiss National Science Foundation professorship to F.H. (PP00P3_150682), an Odysseus Type I grant from The Flanders Research Foundation (FWO) to G.H., FWO project grants to GH (G.0954.16 and G.0306.16) and S.A. (G.0640.13, G.0791.14, and G.0C04.17), Special Research Fund (BOF) KU Leuven grants to S.A. (PF/10/016 and OT/13/103), a Foundation Against Cancer grant to S.A. (2012-F2), an ERC CoG (724226_cis-CONTROL) to S.A., by the Stowers Institute for Medical Research and a National Institutes of Health (NIH) New Innovator Award to J.Z. (1DP2 OD004561-01). J.J. has a PhD Fellowship from the Flemish Agency for Innovation by Science and Technology.

Author Contributions: FH and GH designed the study; SA and JZ contributed methodology; JP, LS, MN, and FH performed the experiments; JJ analyzed the RNA-seq and ChIP-nexus data; JP, JJ, MN, JZ, GH and FH prepared the manuscript; JZ, SA, GH and FH acquired funding.

Competing financial interests: The authors declare no competing financial interests.

Figure Legends:

Figure 1: Activated EGFR can induce either differentiation or proliferation.

(A-D') Wing and (E-H) eye-antennal imaginal discs from late third instar larvae expressing the indicated UAS transgenes with the *dpp-Gal4* driver. (A and E') The expression pattern of *dpp-Gal4* (green). *ex-lacZ* is shown in red (A-D'), Ci antibody marks the MF (red in F-H) and photoreceptor cells are labeled with ELAV antibodies (green in E-H). (B) Homozygous *ex* mutant discs are slightly overgrown and (F) have defects in the movement of the morphogenetic furrow (MF) in the eye. (C) Expression of activated EGFR (EGFR^{top}) in the *dpp* stripe (green) leads to expansion of this region and (G) induces ectopic photoreceptor differentiation. (D and H) The

same construct (EGFR^{top}) induces massive overgrowth in the absence of *ex*. All images are shown at the same scale. Scale bar in (D) is 50 μ m. Genotypes:

A&E: *w; ex^{e1}/+; dpp-Gal4, UAS-GFP^{nls}/+*

B&F: *w; ex^{e1}/ex^{AP50}; dpp-Gal4, UAS-GFP^{nls}/+*

C&G: *w; dpp-Gal4, UAS-GFP^{nls}/ UAS-EGFR^{top}*

D-D’&H: *w; ex^{e1}/ex^{AP50}; dpp-Gal4, UAS-GFP^{nls}/ UAS-EGFR^{top}*

Figure 2: The synergy between the two pathways is at the level of transcriptional regulation.

Third instar eye-antennal imaginal discs (top rows) and male fly heads (bottom row) carrying *eyflp* (expressed only in the head) induced clones of indicated genotypes. Mutant clones are marked by the absence of GFP (green in top, gray in middle panel) or lack of mini-w+ expression (red in bottom panel). (A) *cic^{Q474X}* mutant cells occupy roughly half the tissue and have no effect on photoreceptor differentiation marked by ELAV (red), (B) *ras^{DC408}* mutant clones are small in the larval eye and do not contribute to the adult tissue, (C) further deletion of *cic* rescues the proliferation but not the differentiation defects of *ras^{DC408}* mutant cells, (D) *wts¹⁴⁹* mutant cells over-proliferate and (E) *cic^{Q474X} wts¹⁴⁹* double mutant cells induce overgrowth and many folds in the tissue. The eye field is very small. All discs are from day 5 larvae and are shown at the same magnification. Scale bar in (A) is 100 μ m. Genotypes:

A) *y w eyflp / y w; FRT82B ubiGFP^{nls} / FRT82B cic^{Q474X}*

B) *y w eyflp / y w; FRT82B ubiGFP^{nls} / FRT82B ras^{DC408}*

C) *y w eyflp / y w; FRT82B ubiGFP^{nls} / FRT82B ras^{DC408} cic^{Q474X}*

D) *y w eyflp / y w; FRT82B ubiGFP^{nls} / FRT82B wts¹⁴⁹*

E) *y w eyflp / y w; FRT82B ubiGFP^{nls} / FRT82B cic^{Q474X} wts¹⁴⁹*

Figure 3: Combined mutations in *cic* and *wts* induce tremendous overgrowth and delayed pupation.

(A-B) Control wing and eye discs at the end of larval development. (C-D) Eye and wing discs with *cic^{Q474X} wts¹⁴⁹* double mutant cells in a Minute background. (E) Time course analysis (day 3, 4, 5, 6 and 9) of wing discs with indicated genotypes. Mutations in *wts* lead to delayed pupation. (F) *ubx-FLP, cic wts* discs can grow up to 10 times bigger than a full-grown wild-type wing disc. The graph shows wing area quantification at different time points (n= 3-5 discs per time point per genotype) and in fact underestimates the size of *cic wts* double mutant discs as they form many folds and are on average twice as thick as *wts* discs. All images are at the same magnification. The scale bars in (A) and (E) are 200 μ m. Genotypes:

A-B) $y w; FRT82B M(3) ubiGFP^{nls} / FRT82B cic^{Q474X} wts^{149}$
 C) $y w eyflp / y w; FRT82B M(3) ubiGFP^{nls} / FRT82B cic^{Q474X} wts^{149}$
 D) $y ubxflp / y w; FRT82B M(3) ubiGFP^{nls} / FRT82B cic^{Q474X} wts^{149}$
 E-F) $wt: y ubxflp / y w; FRT82B M(3) ubiGFP^{nls} / FRT82B$
 $wts: y ubxflp / y w; FRT82B M(3) ubiGFP^{nls} / FRT82B wts^{149}$
 $cic: y ubxflp / y w; FRT82B M(3) ubiGFP^{nls} / FRT82B cic^{Q474X}$
 $cic wts: y ubxflp / y w; FRT82B M(3) ubiGFP^{nls} / FRT82B cic^{Q474X} wts^{149}$

Figure 4: RNA-sequencing reveals synergistically regulated genes.

Self Organizing Tree Algorithm (SOTA) found 4 clusters among the 350 upregulated genes in day 5 *cic wts* discs compared to the control discs. Row normalized heat-maps of (A) Wts cluster, (B) known Yki target genes from the Wts cluster. Dilp8 is shown separately as it is most upregulated (28-folds in *wts* discs) and disrupts the visualization of the data when grouped with the other genes. (C) Cic cluster, (D) additive cluster, (E) synergistic cluster and (F) 28 genes from the Wts cluster that are further upregulated in *cic wts* discs (1,3 folds or more). Green bars represent average expression levels.

Figure 5: Pnt and STAT are predicted key regulators of the synergistic genes and are required for the synergistic overgrowth.

(A) iRegulon predicts that three factors, Cic, Pnt and Stat92E regulate the synergistically induced genes. The heat-maps of these 46 synergistic genes are shown in Suppl.Fig.2A. 8 genes whose expression did not stay elevated at day 9 *cic wts* discs were removed from the group as they are unlikely to drive the synergistic phenotype. (B) iRegulon analysis on Cic target genes returns the same network as shown in panel A. The heat-maps of these 19 direct Cic target genes are shown in Suppl.Fig.2B. (C) Heat-map showing the expression levels of JAK-STAT ligands Upds and the transcription factors of Ras signaling, Pnt and Cic in different genotypes and time-points. (D-J) 7-day old wing (top) and eye-antennal (bottom) imaginal discs of indicated genotypes. UAS driven GFP (green) marks the expression domain of the *dpp-Gal4* driver. Nuclei are shown in red marked by DAPI (D-G) or *ex-lacZ* expression (I-J). (H) Quantification of the wing disc areas with our synergistic combination (activated EGFR expression in *ex* mutant background (dark gray)) and upon additional knock-down of *pnt* (light gray) at different time points. We measured at least 6 discs per genotype. For *dpp>EGFR^{top} in ex*; day 5, n=11; day 6, n=10; day 7, n=9. For *dpp>EGFR^{top} + pnt-RNAi in ex*; day 5, n=6; day 6, n=10; day 7,

n=9. All images are shown at the same scale. The scale bar in (F) is 100 μ m.

Genotypes:

D-E) *y w*; *FRT40A ex^{AP50} / FRT40A ex^{e1}*; *UAS-EGFR^{top} / dpp-Gal4, UAS-GFP*

F-G) *y w*; *FRT40A ex^{AP50} UAS-SOCS-36E / FRT40A ex^{e1}*; *UAS-EGFR^{top} / dpp-Gal4, UAS-GFP*

I-J) *y w*; *FRT40A ex^{AP50} / FRT40A ex^{e1}*; *UAS-EGFR^{top} / dpp-Gal4, UAS-GFP, UAS-pnt-RNAi (UAS-pnt-RNAi is BL31936)*

Figure 6: Pointed and Cic are direct Yki-Sd targets.

(A-B) Cic and Pnt expression patterns, detected by antibody stainings, in late third instar wing discs. (C-C') Pnt is derepressed in *cic* mutant clones. (D,F) ChIP-nexus tracks in *pnt* (D) and *cic* (F) genomic regions obtained by overlaying tracks from experimental triplicates. Blue and red tracks correspond to Sd and Cic ChIP data, respectively. Predicted binding motifs for Cic (red), Sd (blue), Pnt (green) and Stat92E (purple) are shown above the tracks. (E-E'') Cic (red in E and E'', gray in E') and ELAV (blue in E'') antibody staining in discs with *wts¹⁴⁹* mutant clones marked by the absence of GFP (green in E) is shown. Cic protein accumulates in interommatidial cells. (G-H') Knocking down *yki* in the posterior compartment leads to a reduction in the compartment size and Cic levels. Hence high, uniform Cic levels require Yki input. The scale bars in C', E and H' are 100 μ m.

Genotypes:

C) *y w hsflp / y w*; *FRT82B ubiGFP^{nlis} / FRT82B cic^{Q474X}*

E) *y w hsflp / y w*; *FRT82B ubiGFP^{nlis} / FRT82B wts¹⁴⁹*

G) *y w*; *en-Gal4 / +*

H) *y w*; *en-Gal4 / +*; *UAS-Yki-RNAi / +*

Figure 7: Model of the transcriptional interaction between the Hippo and Ras pathways.

The Hippo pathway effectors Yki-Sd regulate the expression of the Pnt and Cic transcription factors of the Ras pathway. The induction of Pnt regulates the sensitivity of a cell to Ras signaling, while the induction of Cic increases the threshold required for productive output. As a result, Cic target genes and synergy are only fully activated when Cic is removed and Yki is simultaneously activated. Thus, the activity of the Hippo pathway together with the repressor Cic provide parallel breaks that limit Ras signaling output and prevent hyperproliferation and cellular transformation. Blue highlights the interactions revealed in this study.

Figure S1: Different combinations of Hippo loss and Ras gain-of-function induce synergistic overgrowth.

(A) Regardless of which level of signaling the two pathways are modulated, the synergistic overgrowth is observed. Photoreceptors are marked by ELAV staining in blue in all panels. The green signal in the middle and the right panel shows the GFP expression under *dpp-Gal4*. The scale bar is 50uM. Genotypes:

Left) *y w; FRT40A ex^{BQ} / FRT40A ex^{e1}; UAS-Ras^{V12} / dpp-Gal4, UAS-GFP*

Middle) *y w; FRT40A ex^{BQ} / FRT40A ex^{e1}; UAS-Raf^{GOF} / dpp-Gal4, UAS-GFP*

Right) *y w; UAS-EGFR^{top} / +; UAS-Yki / dpp-Gal4, UAS-GFP*

(B-C) Yki overexpression in combination with *cic* knock-down induces synergistic overgrowth. Representative discs of indicated genotypes (B) and quantification of the GFP-positive areas as a percentage of the whole disc area are shown (C). Error bars represent standard deviation. Discs where *cic* is knocked down are slightly smaller (86% of normal size) with a slightly wider Ptc stripe. In discs where Yki is overexpressed, the Ptc stripe occupies more than a quarter of the whole disc. Additional *cic* knock-down further expands the Ptc stripe which now occupies a third of the disc. All discs shown are from day 5. *Ptc > Yki + cic-RNAi* larvae have extended larval life by an additional 2 days, but the discs do not further grow. Anterior is to the left and the scale bar is 100uM.

Genotypes:

ptc > GFP : y w; ptc-Gal4, UAS-GFP / CyO

ptc > cic-RNAi : y w; ptc-Gal4, UAS-GFP / UAS-cic-RNAi (VDRC line 103805)

ptc > Yki : y w; ptc-Gal4, UAS-GFP / + ; UAS-Yki / +

ptc > Yki + cic-RNAi : y w; ptc-Gal4, UAS-GFP / UAS-cic-RNAi ; UAS-Yki / +

Figure S2: Heatmaps for synergistic and Cic target genes. Upd transcription is under Sd and Cic control.

Row normalized heat-maps showing expression profiles of synergistically induced genes (A) and direct Cic target genes (B) in day 5 discs of indicated genotypes. (C) ChIP-nexus peaks (Sd in blue and Cic in red) and motifs (Sd in blue and Cic in red) in the Upd region suggest direct binding of Cic and Sd.

Figure S3: Expression patterns and regulation of Pnt and Yan.

(A) Pnt and Yan are expressed posterior to the morphogenetic furrow in the eye discs. (B) Cic expression pattern is complementary to that of Pnt and Yan in eye discs. (C) Yan protein is not detected in wing discs. (D) Pnt antibody staining (gray) reflects the Ras activity pattern in a third instar wing imaginal disc. (E) Pnt pattern is

weaker in an *ex* disc likely due to higher Cic levels. (F-F') Pnt is de/repressed (gray F, red in F') in *cic* mutant cells marked by the absence of GFP (green in F') in an *ex* disc. (G-G') Pnt protein levels (gray G, red in G') are highly elevated in *cic wts* mutant cells marked by the absence of GFP and the pattern is lost. All images are shown at the same scale. Genotypes:

E) *y w / w; FRT40A ex^{e1} / FRT40A ex^{AP50}*

F) *y w hsflp / w; FRT40A ex^{e1} / FRT40A ex^{AP50}; FRT82B ubiGFP / FRT82B cic^{Q474X}*

G) *y w hsflp / y w; FRT82B ubiGFP^{nls} / FRT82B cic^{Q474X} wts¹⁴⁹*

Figure S4: Ras regulates Yki activity, but Cic does not.

Late third instar imaginal discs that carry (A) EGFR^{top} or (B) Ras overexpression clones marked by GFP co-expression in green and stained with β-gal antibodies to reveal *ex-lacZ* expression in red (gray in A' and B'). Within the pouch region, most clones of cells with activated EGFR/Ras signaling showed a cell autonomous upregulation of *ex-lacZ* expression (arrows). On the other hand, clones outside the pouch area (arrowheads) had either no effect or only boundary effects on *ex-lacZ* levels. (C) *cic* mutant clones marked by lack of GFP expression do not modulate *ex-lacZ* expression (red in C, gray in C'). (D) *cic* mutant clones overgrow and form folds (arrowheads) in *ex^{e1}/ex^{AP50}* mutant background, but do not affect *ex-lacZ* expression (red in D, gray in D'). (E-F) Ex protein levels are not affected by loss of *cic* even in a *wts* mutant disc where they overgrow and display synergy. All scale bars are 100u.

Full genotypes:

A) *y w hsflp / w; FRT40A ex^{e1}/+; UAS-EGFR^{top} / act < CD2 < Gal4, UAS-GFP*

B) *y w hsflp / w; FRT40A ex^{e1}/+; UAS-Ras / act < CD2 < Gal4, UAS-GFP*

C) *y w hsflp / w; FRT40A ex^{e1}/+; FRT82B ubiGFP / FRT82B cic^{Q474X}*

D) *y w hsflp / w; FRT40A ex^{e1} / FRT40A ex^{AP50}; FRT82B ubiGFP / FRT82B cic^{Q474X}*

E) *y w hsflp / w; FRT82B wts^{P2} ubiGFP / FRT82B wts¹⁴⁹*

F) *y w hsflp / w; FRT82B wts^{P2} ubiGFP / FRT82B cic^{Q474X} wts¹⁴⁹*

Figure S5: The differentiation program is shut down in *cic wts* mutant cells.

(A) Row normalized heat-map showing expression profiles of components and target genes for developmental pathways in day 5 discs of indicated genotypes. Pathway readouts for Dpp, Notch, Wg and Hh signaling are down regulated in *cic wts* mutant discs. (B) Eye discs from indicated genotypes and ages. Similar to Figure 2, but the discs are allowed to grow to their maximum potential. *wts* mutant cells (marked by the absence of GFP in green) can differentiate into photoreceptors (red), but are positioned further apart from each other due to the increased number of

interommatidial cells. Photoreceptor rosettes are often incomplete in *cic wts* mutant areas. The scale bar in (B) is 50 μ m. Genotypes:

wt: *y w eyflp / y w; FRT82B ubiGFP^{nls} / FRT82B*

wts: *y w eyflp / y w; FRT82B ubiGFP^{nls} / FRT82B wts¹⁴⁹*

cicwts: *y w eyflp / y w; FRT82B ubiGFP^{nls} / FRT82B cic^{Q474X} wts¹⁴⁹*

References

- Affolter, M. and Basler, K. (2007) 'The Decapentaplegic morphogen gradient: from pattern formation to growth regulation', *Nat Rev Genet*, 8(9), pp. 663-74.
- Amoyel, M., Anderson, A. M. and Bach, E. A. (2014) 'JAK/STAT pathway dysregulation in tumors: a Drosophila perspective', *Semin Cell Dev Biol*, 28, pp. 96-103.
- Anders, S., Pyl, P. T. and Huber, W. (2015) 'HTSeq--a Python framework to work with high-throughput sequencing data', *Bioinformatics*, 31(2), pp. 166-9.
- Atkins, M., Potier, D., Romanelli, L., Jacobs, J., Mach, J., Hamaratoglu, F., Aerts, S. and Halder, G. (2016) 'An Ectopic Network of Transcription Factors Regulated by Hippo Signaling Drives Growth and Invasion of a Malignant Tumor Model', *Curr Biol*, 26(16), pp. 2101-13.
- Ballester, R., Marchuk, D., Boguski, M., Saulino, A., Letcher, R., Wigler, M. and Collins, F. (1990) 'The NF1 locus encodes a protein functionally related to mammalian GAP and yeast IRA proteins', *Cell*, 63(4), pp. 851-9.
- Barry, E. R. and Camargo, F. D. (2013) 'The Hippo superhighway: signaling crossroads converging on the Hippo/Yap pathway in stem cells and development', *Curr Opin Cell Biol*, 25(2), pp. 247-53.
- Boone, E., Colombani, J., Andersen, D. S. and Léopold, P. (2016) 'The Hippo signalling pathway coordinates organ growth and limits developmental variability by controlling *dilp8* expression', *Nat Commun*, 7, pp. 13505.
- Brand, A. H. and Perrimon, N. (1994) 'Raf acts downstream of the EGF receptor to determine dorsoventral polarity during Drosophila oogenesis', *Genes Dev*, 8(5), pp. 629-39.
- Brumby, A. M. and Richardson, H. E. (2003) 'scribble mutants cooperate with oncogenic Ras or Notch to cause neoplastic overgrowth in Drosophila', *Embo J*, 22(21), pp. 5769-79.
- Buchberg, A. M., Cleveland, L. S., Jenkins, N. A. and Copeland, N. G. (1990) 'Sequence homology shared by neurofibromatosis type-1 gene and IRA-1 and IRA-2 negative regulators of the RAS cyclic AMP pathway', *Nature*, 347(6290), pp. 291-4.
- Bunker, B. D., Nellimoottil, T. T., Boileau, R. M., Classen, A. K. and Bilder, D. (2015) 'The transcriptional response to tumorigenic polarity loss in Drosophila', *Elife*, 4.
- Burgess, A. W. (2008) 'EGFR family: structure physiology signalling and therapeutic targets', *Growth Factors*, 26(5), pp. 263-74.
- Butchar, J. P., Cain, D., Manivannan, S. N., McCue, A. D., Bonanno, L., Halula, S., Truesdell, S., Austin, C. L., Jacobsen, T. L. and Simcox, A. (2012) 'New negative feedback regulators of Egrf signaling in Drosophila', *Genetics*, 191(4), pp. 1213-26.
- Casci, T., Vinós, J. and Freeman, M. (1999) 'Sprouty, an intracellular inhibitor of Ras signaling', *Cell*, 96(5), pp. 655-65.
- Chabu, C., Li, D. M. and Xu, T. (2017) 'EGFR/ARF6 regulation of Hh signalling stimulates oncogenic Ras tumour overgrowth', *Nat Commun*, 8, pp. 14688.

- Colombani, J., Polesello, C., Josué, F. and Tapon, N. (2006) 'Dmp53 activates the Hippo pathway to promote cell death in response to DNA damage', *Curr Biol*, 16(14), pp. 1453-8.
- Davie, K., Jacobs, J., Atkins, M., Potier, D., Christiaens, V., Halder, G. and Aerts, S. (2015) 'Discovery of transcription factors and regulatory regions driving in vivo tumor development by ATAC-seq and FAIRE-seq open chromatin profiling', *PLoS Genet*, 11(2), pp. e1004994.
- Dopazo, J. and Carazo, J. M. (1997) 'Phylogenetic reconstruction using an unsupervised growing neural network that adopts the topology of a phylogenetic tree', *J Mol Evol*, 44(2), pp. 226-33.
- Feng, J., Liu, T. and Zhang, Y. (2011) 'Using MACS to identify peaks from ChIP-Seq data', *Curr Protoc Bioinformatics*, Chapter 2, pp. Unit 2.14.
- Forbes, S. A., Beare, D., Gunasekaran, P., Leung, K., Bindal, N., Boutselakis, H., Ding, M., Bamford, S., Cole, C., Ward, S., Kok, C. Y., Jia, M., De, T., Teague, J. W., Stratton, M. R., McDermott, U. and Campbell, P. J. (2015) 'COSMIC: exploring the world's knowledge of somatic mutations in human cancer', *Nucleic Acids Res*, 43(Database issue), pp. D805-11.
- Garcia-Rendueles, M. E., Ricarte-Filho, J. C., Untch, B. R., Landa, I., Knauf, J. A., Voza, F., Smith, V. E., Ganly, I., Taylor, B. S., Persaud, Y., Oler, G., Fang, Y., Jhanwar, S. C., Viale, A., Heguy, A., Huberman, K. H., Giancotti, F., Ghossein, R. and Fagin, J. A. (2015) 'NF2 Loss Promotes Oncogenic RAS-Induced Thyroid Cancers via YAP-Dependent Transactivation of RAS Proteins and Sensitizes Them to MEK Inhibition', *Cancer Discov*, 5(11), pp. 1178-93.
- Garoia, F., Grifoni, D., Trotta, V., Guerra, D., Pezzoli, M. C. and Cavicchi, S. (2005) 'The tumor suppressor gene fat modulates the EGFR-mediated proliferation control in the imaginal tissues of *Drosophila melanogaster*', *Mech Dev*, 122(2), pp. 175-87.
- Gaujoux, R. and Seoighe, C. (2010) 'A flexible R package for nonnegative matrix factorization', *BMC Bioinformatics*, 11, pp. 367.
- Glise, B., Miller, C. A., Crozatier, M., Halbisen, M. A., Wise, S., Olson, D. J., Vincent, A. and Blair, S. S. (2005) 'Shifted, the *Drosophila* ortholog of Wnt inhibitory factor-1, controls the distribution and movement of Hedgehog', *Dev Cell*, 8(2), pp. 255-66.
- Golembo, M., Schweitzer, R., Freeman, M. and Shilo, B. Z. (1996) 'Argos transcription is induced by the *Drosophila* EGF receptor pathway to form an inhibitory feedback loop', *Development*, 122(1), pp. 223-30.
- Gorfinkiel, N., Sierra, J., Callejo, A., Ibañez, C. and Guerrero, I. (2005) 'The *Drosophila* ortholog of the human Wnt inhibitor factor Shifted controls the diffusion of lipid-modified Hedgehog', *Dev Cell*, 8(2), pp. 241-53.
- Grusche, F. A., Richardson, H. E. and Harvey, K. F. (2010) 'Upstream regulation of the hippo size control pathway', *Curr Biol*, 20(13), pp. R574-82.
- Halder, G. and Johnson, R. L. (2011) 'Hippo signaling: growth control and beyond', *Development*, 138(1), pp. 9-22.
- Hamaratoglu, F., de Lachapelle, A. M., Pyrowolakis, G., Bergmann, S. and Affolter, M. (2011) 'Dpp signaling activity requires pentagone to scale with tissue size in the growing *Drosophila* wing imaginal disc', *PLoS biology*, 9(10), pp. e1001182.
- Hamaratoglu, F., Willecke, M., Kango-Singh, M., Nolo, R., Hyun, E., Tao, C., Jafar-Nejad, H. and Halder, G. (2006) 'The tumour-suppressor genes NF2/Merlin and Expanded act through Hippo signalling to regulate cell proliferation and apoptosis', *Nat Cell Biol*, 8(1), pp. 27-36.
- Hariharan, I. K. (2015) 'Organ Size Control: Lessons from *Drosophila*', *Dev Cell*, 34(3), pp. 255-65.

- Harvey, K. F., Zhang, X. and Thomas, D. M. (2013) 'The Hippo pathway and human cancer', *Nat Rev Cancer*, 13(4), pp. 246-57.
- He, Q., Johnston, J. and Zeitlinger, J. (2015) 'ChIP-nexus enables improved detection of in vivo transcription factor binding footprints', *Nat Biotechnol*, 33(4), pp. 395-401.
- Herrero, J., Valencia, A. and Dopazo, J. (2001) 'A hierarchical unsupervised growing neural network for clustering gene expression patterns', *Bioinformatics*, 17(2), pp. 126-36.
- Hong, X., Nguyen, H. T., Chen, Q., Zhang, R., Hagman, Z., Voorhoeve, P. M. and Cohen, S. M. (2014) 'Opposing activities of the Ras and Hippo pathways converge on regulation of YAP protein turnover', *EMBO J*, 33(21), pp. 2447-57.
- Ikmi, A., Gaertner, B., Seidel, C., Srivastava, M., Zeitlinger, J. and Gibson, M. C. (2014) 'Molecular evolution of the Yap/Yorkie proto-oncogene and elucidation of its core transcriptional program', *Mol Biol Evol*, 31(6), pp. 1375-90.
- Imrichová, H., Hulselmans, G., Atak, Z. K., Potier, D. and Aerts, S. (2015) 'i-cisTarget 2015 update: generalized cis-regulatory enrichment analysis in human, mouse and fly', *Nucleic Acids Res*, 43(W1), pp. W57-64.
- Janky, R., Verfaillie, A., Imrichová, H., Van de Sande, B., Standaert, L., Christiaens, V., Hulselmans, G., Hertzen, K., Naval Sanchez, M., Potier, D., Svetlichnyy, D., Kalender Atak, Z., Fiers, M., Marine, J. C. and Aerts, S. (2014) 'iRegulon: from a gene list to a gene regulatory network using large motif and track collections', *PLoS Comput Biol*, 10(7), pp. e1003731.
- Jiménez, G., Shvartsman, S. Y. and Paroush, Z. (2012) 'The Capicua repressor--a general sensor of RTK signaling in development and disease', *J Cell Sci*, 125(Pt 6), pp. 1383-91.
- Jin, Y., Ha, N., Forés, M., Xiang, J., Gläßer, C., Maldera, J., Jiménez, G. and Edgar, B. A. (2015) 'EGFR/Ras Signaling Controls Drosophila Intestinal Stem Cell Proliferation via Capicua-Regulated Genes', *PLoS Genet*, 11(12), pp. e1005634.
- Justice, R. W., Zilian, O., Woods, D. F., Noll, M. and Bryant, P. J. (1995) 'The Drosophila tumor suppressor gene warts encodes a homolog of human myotonic dystrophy kinase and is required for the control of cell shape and proliferation', *Genes Dev*, 9(5), pp. 534-46.
- Kagey, J. D., Brown, J. A. and Moberg, K. H. (2012) 'Regulation of Yorkie activity in Drosophila imaginal discs by the Hedgehog receptor gene patched', *Mech Dev*, 129(9-12), pp. 339-49.
- Kandoth, C., McLellan, M. D., Vandin, F., Ye, K., Niu, B., Lu, C., Xie, M., Zhang, Q., McMichael, J. F., Wyczalkowski, M. A., Leiserson, M. D., Miller, C. A., Welch, J. S., Walter, M. J., Wendl, M. C., Ley, T. J., Wilson, R. K., Raphael, B. J. and Ding, L. (2013) 'Mutational landscape and significance across 12 major cancer types', *Nature*, 502(7471), pp. 333-9.
- Karaman, R. and Halder, G. (2017) 'Cell Junctions in Hippo Signaling', *Cold Spring Harb Perspect Biol*.
- Kim, D., Pertea, G., Trapnell, C., Pimentel, H., Kelley, R. and Salzberg, S. L. (2013) 'TopHat2: accurate alignment of transcriptomes in the presence of insertions, deletions and gene fusions', *Genome Biol*, 14(4), pp. R36.
- Kleinschmit, A., Takemura, M., Dejima, K., Choi, P. Y. and Nakato, H. (2013) 'Drosophila heparan sulfate 6-O-endosulfatase Sulf1 facilitates wingless (Wg) protein degradation', *J Biol Chem*, 288(7), pp. 5081-9.
- Koontz, L. M., Liu-Chittenden, Y., Yin, F., Zheng, Y., Yu, J., Huang, B., Chen, Q., Wu, S. and Pan, D. (2013) 'The Hippo effector Yorkie controls normal tissue growth by antagonizing scalloped-mediated default repression', *Dev Cell*, 25(4), pp. 388-401.

- Lee, K. P., Lee, J. H., Kim, T. S., Kim, T. H., Park, H. D., Byun, J. S., Kim, M. C., Jeong, W. I., Calvisi, D. F., Kim, J. M. and Lim, D. S. (2010) 'The Hippo-Salvador pathway restrains hepatic oval cell proliferation, liver size, and liver tumorigenesis', *Proc Natl Acad Sci U S A*, 107(18), pp. 8248-53.
- Legoff, L., Rouault, H. and Lecuit, T. (2013) 'A global pattern of mechanical stress polarizes cell divisions and cell shape in the growing *Drosophila* wing disc', *Development*, 140(19), pp. 4051-9.
- Lemmon, M. A. and Schlessinger, J. (2010) 'Cell signaling by receptor tyrosine kinases', *Cell*, 141(7), pp. 1117-34.
- Lin, L., Sabnis, A. J., Chan, E., Olivas, V., Cade, L., Pazarentzos, E., Asthana, S., Neel, D., Yan, J. J., Lu, X., Pham, L., Wang, M. M., Karachaliou, N., Cao, M. G., Manzano, J. L., Ramirez, J. L., Torres, J. M., Buttitta, F., Rudin, C. M., Collisson, E. A., Algazi, A., Robinson, E., Osman, I., Muñoz-Couselo, E., Cortes, J., Frederick, D. T., Cooper, Z. A., McMahon, M., Marchetti, A., Rosell, R., Flaherty, K. T., Wargo, J. A. and Bivona, T. G. (2015) 'The Hippo effector YAP promotes resistance to RAF- and MEK-targeted cancer therapies', *Nat Genet*, 47(3), pp. 250-6.
- Love, M. I., Huber, W. and Anders, S. (2014) 'Moderated estimation of fold change and dispersion for RNA-seq data with DESeq2', *Genome Biol*, 15(12), pp. 550.
- Lu, L., Li, Y., Kim, S. M., Bossuyt, W., Liu, P., Qiu, Q., Wang, Y., Halder, G., Finegold, M. J., Lee, J. S. and Johnson, R. L. (2010) 'Hippo signaling is a potent in vivo growth and tumor suppressor pathway in the mammalian liver', *Proc Natl Acad Sci U S A*, 107(4), pp. 1437-42.
- Ma, X., Chen, Y., Xu, W., Wu, N., Li, M., Cao, Y., Wu, S., Li, Q. and Xue, L. (2015) 'Impaired Hippo signaling promotes Rho1-JNK-dependent growth', *Proc Natl Acad Sci U S A*, 112(4), pp. 1065-70.
- Mao, Y., Tournier, A. L., Hoppe, A., Kester, L., Thompson, B. J. and Tapon, N. (2013) 'Differential proliferation rates generate patterns of mechanical tension that orient tissue growth', *EMBO J*, 32(21), pp. 2790-803.
- Martin, G. A., Viskochil, D., Bollag, G., McCabe, P. C., Crosier, W. J., Haubruck, H., Conroy, L., Clark, R., O'Connell, P. and Cawthon, R. M. (1990) 'The GAP-related domain of the neurofibromatosis type 1 gene product interacts with ras p21', *Cell*, 63(4), pp. 843-9.
- Marygold, S. J., Coelho, C. M. and Leivers, S. J. (2005) 'Genetic analysis of RpL38 and RpL5, two minute genes located in the centric heterochromatin of chromosome 2 of *Drosophila melanogaster*', *Genetics*, 169(2), pp. 683-95.
- Mayrhofer, M., Gourain, V., Reischl, M., Affaticati, P., Jenett, A., Joly, J. S., Benelli, M., Demichelis, F., Poliani, P. L., Sieger, D. and Mione, M. (2017) 'A novel brain tumour model in zebrafish reveals the role of YAP activation in MAPK- and PI3K-induced malignant growth', *Dis Model Mech*, 10(1), pp. 15-28.
- Morata, G. and Ripoll, P. (1975) 'Minutes: mutants of *drosophila* autonomously affecting cell division rate', *Dev Biol*, 42(2), pp. 211-21.
- Neto-Silva, R. M., de Beco, S. and Johnston, L. A. (2010) 'Evidence for a growth-stabilizing regulatory feedback mechanism between Myc and Yorkie, the *Drosophila* homolog of Yap', *Dev Cell*, 19(4), pp. 507-20.
- Okamoto, N., Nakamori, R., Murai, T., Yamauchi, Y., Masuda, A. and Nishimura, T. (2013) 'A secreted decoy of InR antagonizes insulin/IGF signaling to restrict body growth in *Drosophila*', *Genes Dev*, 27(1), pp. 87-97.
- Pagliarini, R. A. and Xu, T. (2003) 'A genetic screen in *Drosophila* for metastatic behavior', *Science*, 302(5648), pp. 1227-31.
- Pan, D. (2007) 'Hippo signaling in organ size control', *Genes Dev*, 21(8), pp. 886-97.
- Pan, D. (2010) 'The hippo signaling pathway in development and cancer', *Dev Cell*, 19(4), pp. 491-505.

- Park, G. S., Oh, H., Kim, M., Kim, T., Johnson, R. L., Irvine, K. D. and Lim, D. S. (2016) 'An evolutionarily conserved negative feedback mechanism in the Hippo pathway reflects functional difference between LATS1 and LATS2', *Oncotarget*, 7(17), pp. 24063-75.
- Pearson, H. B., Perez-Mancera, P. A., Dow, L. E., Ryan, A., Tennstedt, P., Bogani, D., Elsum, I., Greenfield, A., Tuveson, D. A., Simon, R. and Humbert, P. O. (2011) 'SCRIB expression is deregulated in human prostate cancer, and its deficiency in mice promotes prostate neoplasia', *J Clin Invest*, 121(11), pp. 4257-67.
- Piccolo, S., Dupont, S. and Cordenonsi, M. (2014) 'The biology of YAP/TAZ: hippo signaling and beyond', *Physiol Rev*, 94(4), pp. 1287-312.
- Queenan, A. M., Ghabrial, A. and Schüpbach, T. (1997) 'Ectopic activation of torpedo/Egfr, a Drosophila receptor tyrosine kinase, dorsalizes both the eggshell and the embryo', *Development*, 124(19), pp. 3871-80.
- Reddy, B. V. and Irvine, K. D. (2013) 'Regulation of Hippo signaling by EGFR-MAPK signaling through Ajuba family proteins', *Dev Cell*, 24(5), pp. 459-71.
- Richardson, H. E. and Portela, M. (2017) 'Tissue growth and tumorigenesis in Drosophila: cell polarity and the Hippo pathway', *Curr Opin Cell Biol*, 48, pp. 1-9.
- Roch, F., Jiménez, G. and Casanova, J. (2002) 'EGFR signalling inhibits Capicua-dependent repression during specification of Drosophila wing veins', *Development*, 129(4), pp. 993-1002.
- Saeed, A. I., Sharov, V., White, J., Li, J., Liang, W., Bhagabati, N., Braisted, J., Klapa, M., Currier, T., Thiagarajan, M., Sturn, A., Snuffin, M., Rezantsev, A., Popov, D., Ryltsov, A., Kostukovich, E., Borisovsky, I., Liu, Z., Vinsavich, A., Trush, V. and Quackenbush, J. (2003) 'TM4: a free, open-source system for microarray data management and analysis', *Biotechniques*, 34(2), pp. 374-8.
- Schnidar, H., Eberl, M., Klingler, S., Mangelberger, D., Kasper, M., Hauser-Kronberger, C., Regl, G., Kroismayr, R., Moriggl, R., Sibilina, M. and Aberger, F. (2009) 'Epidermal growth factor receptor signaling synergizes with Hedgehog/GLI in oncogenic transformation via activation of the MEK/ERK/JUN pathway', *Cancer Res*, 69(4), pp. 1284-92.
- Scholz, H., Sadlowski, E., Klaes, A. and Klämbt, C. (1997) 'Control of midline glia development in the embryonic Drosophila CNS', *Mech Dev*, 64(1-2), pp. 137-51.
- Schweitzer, R., Howes, R., Smith, R., Shilo, B. Z. and Freeman, M. (1995) 'Inhibition of Drosophila EGF receptor activation by the secreted protein Argos', *Nature*, 376(6542), pp. 699-702.
- Shilo, B. Z. (2014) 'The regulation and functions of MAPK pathways in Drosophila', *Methods*, 68(1), pp. 151-9.
- Shwartz, A., Yogev, S., Schejter, E. D. and Shilo, B. Z. (2013) 'Sequential activation of ETS proteins provides a sustained transcriptional response to EGFR signaling', *Development*, 140(13), pp. 2746-54.
- Song, H., Mak, K. K., Topol, L., Yun, K., Hu, J., Garrett, L., Chen, Y., Park, O., Chang, J., Simpson, R. M., Wang, C. Y., Gao, B., Jiang, J. and Yang, Y. (2010) 'Mammalian Mst1 and Mst2 kinases play essential roles in organ size control and tumor suppression', *Proc Natl Acad Sci U S A*, 107(4), pp. 1431-6.
- Stec, W., Vidal, O. and Zeidler, M. P. (2013) 'Drosophila SOCS36E negatively regulates JAK/STAT pathway signaling via two separable mechanisms', *Mol Biol Cell*, 24(18), pp. 3000-9.
- Stemerdink, C. and Jacobs, J. R. (1997) 'Argos and Spitz group genes function to regulate midline glial cell number in Drosophila embryos', *Development*, 124(19), pp. 3787-96.

- Tomasetti, C., Marchionni, L., Nowak, M. A., Parmigiani, G. and Vogelstein, B. (2015) 'Only three driver gene mutations are required for the development of lung and colorectal cancers', *Proc Natl Acad Sci U S A*, 112(1), pp. 118-23.
- Tseng, A. S., Tapon, N., Kanda, H., Cigizoglu, S., Edelman, L., Pellock, B., White, K. and Hariharan, I. K. (2007) 'Capicua regulates cell proliferation downstream of the receptor tyrosine kinase/ras signaling pathway', *Curr Biol*, 17(8), pp. 728-33.
- Uhlirva, M. and Bohmann, D. (2006) 'JNK- and Fos-regulated Mmp1 expression cooperates with Ras to induce invasive tumors in *Drosophila*', *EMBO J*, 25(22), pp. 5294-304.
- Vakiani, E. and Solit, D. B. (2011) 'KRAS and BRAF: drug targets and predictive biomarkers', *J Pathol*, 223(2), pp. 219-29.
- Wojcinski, A., Nakato, H., Soula, C. and Glise, B. (2011) 'DSulfatase-1 fine-tunes Hedgehog patterning activity through a novel regulatory feedback loop', *Dev Biol*, 358(1), pp. 168-80.
- Wu, M., Pastor-Pareja, J. C. and Xu, T. (2010) 'Interaction between Ras(V12) and scribbled clones induces tumour growth and invasion', *Nature*, 463(7280), pp. 545-8.
- Xia, M. and Land, H. (2007) 'Tumor suppressor p53 restricts Ras stimulation of RhoA and cancer cell motility', *Nat Struct Mol Biol*, 14(3), pp. 215-23.
- Xu, G. F., Lin, B., Tanaka, K., Dunn, D., Wood, D., Gesteland, R., White, R., Weiss, R. and Tamanoi, F. (1990) 'The catalytic domain of the neurofibromatosis type 1 gene product stimulates ras GTPase and complements ira mutants of *S. cerevisiae*', *Cell*, 63(4), pp. 835-41.
- Xu, T., Wang, W., Zhang, S., Stewart, R. A. and Yu, W. (1995) 'Identifying tumor suppressors in genetic mosaics: the *Drosophila* *lats* gene encodes a putative protein kinase', *Development*, 121(4), pp. 1053-63.
- Yan, D. and Lin, X. (2009) 'Shaping morphogen gradients by proteoglycans', *Cold Spring Harb Perspect Biol*, 1(3), pp. a002493.
- Yang, L. and Baker, N. E. (2001) 'Role of the EGFR/Ras/Raf pathway in specification of photoreceptor cells in the *Drosophila* retina', *Development*, 128(7), pp. 1183-91.
- Yang, L. and Baker, N. E. (2003) 'Cell cycle withdrawal, progression, and cell survival regulation by EGFR and its effectors in the differentiating *Drosophila* eye', *Dev Cell*, 4(3), pp. 359-69.
- You, J., Belenkaya, T. and Lin, X. (2011) 'Sulfated is a negative feedback regulator of wingless in *Drosophila*', *Dev Dyn*, 240(3), pp. 640-8.
- Zanconato, F., Cordenonsi, M. and Piccolo, S. (2016) 'YAP/TAZ at the Roots of Cancer', *Cancer Cell*, 29(6), pp. 783-803.
- Zhou, D., Conrad, C., Xia, F., Park, J. S., Payer, B., Yin, Y., Lauwers, G. Y., Thasler, W., Lee, J. T., Avruch, J. and Bardeesy, N. (2009) 'Mst1 and Mst2 maintain hepatocyte quiescence and suppress hepatocellular carcinoma development through inactivation of the Yap1 oncogene', *Cancer Cell*, 16(5), pp. 425-38.
- Ziosi, M., Baena-López, L. A., Grifoni, D., Foldi, F., Pession, A., Garoia, F., Trotta, V., Bellosta, P. and Cavicchi, S. (2010) 'dMyc functions downstream of Yorkie to promote the supercompetitive behavior of hippo pathway mutant cells', *PLoS Genet*, 6(9), pp. e1001140.
- Zoranovic, T., Grmai, L. and Bach, E. A. (2013) 'Regulation of proliferation, cell competition, and cellular growth by the *Drosophila* JAK-STAT pathway', *JAKSTAT*, 2(3), pp. e25408.

STAR Methods:

CONTACT FOR REAGENT AND RESOURCE SHARING

Requests for resources and reagents should be directed to Fisun Hamaratoglu (fisun.hamaratoglu@unil.ch)

EXPERIMENTAL MODEL AND SUBJECT DETAILS

Drosophila melanogaster were grown on standard fly medium and kept in 26°C incubators.

METHOD DETAILS

Immunohistochemistry

Standard protocols were followed for immunohistochemistry (as detailed in (Hamaratoglu et al., 2011)). Antibodies used were: m- β -gal (1:2000, Promega), r-ELAV (1:1500, DSHB-7E8A10), m-Yan (1:10, DSHB-8B12H9), r-Ci (1:150, Robert A. Holmgren), rb-Pnt (1:2000), m-dp-ERK (1:5000, Benny Shilo), gp-Cic (1:300, Iswar Hariharan).

Antibody production

Antibodies against Pnt and Cic were produced by GenScript. They were antigen affinity purified and resuspended in PBS pH 7.4 / 0.02% sodium azide at the following concentrations: anti-rabbit-Pnt = 2.622 mg/ml, anti-rabbit-Cic = 1.715 mg/ml. Pnt C-term half (last 298 aas), that is common to all isoforms, was used as an epitope and the antibody recognizes overexpressed Pnt-P1 and Pnt-P2. For Cic, a C-term small peptide (NDSMDDDTPFDYRK) was used to generate a peptide antibody.

RNA-seq sample preparation and sequencing

Wing discs were collected from 12-35 larvae under sterile conditions and immediately lysed. Genotypes used were: wt, day 5 (y w ubxflp/ y w; FRT82B M(3) ubiGFP/ FRT 82B), *cic*, day 5 (y w ubxflp/ y w; FRT82B M(3) ubiGFP/ FRT 82B *cic*^{Q474X}), *wts*, day 5 and day 9 (y w ubxflp/ y w; FRT82B M(3) ubiGFP/ FRT 82B *wts*¹⁴⁹), *cic wts*, day 5 and day 9 (y w ubxflp/ y w; FRT82B M(3) ubiGFP/ FRT 82B *cic*^{Q474X} *wts*¹⁴⁹). RNA extraction was done using Ambion RNAqueous Micro kit. 500ng total RNA and Illumina TruSeq mRNA Library Prep reagents were used according to the protocol recommended by the manufacturer for library preparation and the sequencing was done using Illumina HiSeq2500.

Isolation of chromatin from imaginal discs

We used larvae of following genotypes: wild-type control (y w ubxflp/ y w; FRT82B M(3) ubiGFP/ FRT 82B), 500 wing discs/ sample; *wts* mutant discs from day9 giant larvae (y w ubxflp/ y w; FRT82B M(3) ubiGFP/ FRT 82B *wts*¹⁴⁹), 100 wing discs/ sample; *cic wts* mutant discs from day9 giant larvae (y w ubxflp/ y w; FRT82B M(3) ubiGFP/ FRT 82B *cic*^{Q474X} *wts*¹⁴⁹), 100 wing discs/ sample.

Third instar larvae were dissected in cold PBS and imaginal disc complexes (anterior one third of the larvae after removing the fat body and salivary glands) were fixed in 1 ml fixation buffer (50 mM 4-(2-hydroxyethyl)-1-piperazineethanesulfonic acid [HEPES], pH 7.5; 1 mM ethylenediaminetetraacetic acid [EDTA]; 0.5 mM ethylene glycol tetraacetic acid [EGTA]; 100 mM NaCl; 2% formaldehyde) for 30 min at room temperature. Fixed disc complexes were washed 3x fast and 2x 20 minutes with PBST (PBS, pH 7.4; 0.1% Triton X-100; 0.1% Tween-20), and were stored at 4°C until enough discs were obtained. 100-500 wing discs were dissected away from the cuticle and resuspended in buffer A2 (15 mM HEPES, pH 7.5; 140 mM NaCl; 1 mM EDTA; 0.5 mM EGTA; 1% Triton X-100; 0.1% sodium deoxycholate; 0.1 % sodium dodecyl sulfate [SDS]; 0.5 % *N*-lauroylsarcosine; 1× Roche complete protease inhibitor cocktail, cat. no. 5056489001). Tubes were flash frozen in liquid nitrogen and stored at -80°C. Imaginal discs were pooled to reach 500 wt discs (or 100 mutant), and sonication was performed in a Bioruptor sonicator for 5 min (30 s on/off cycle at the “high” setting) in buffer A2. Following centrifugation (16,000 × g; 10 min at 4 °C), the supernatant containing soluble chromatin was transferred to fresh tubes, and used for ChIP-nexus.

ChIP-nexus

20 µg antibody (rb-Sd (Ikmi et al., 2014) or rb-Cic) was incubated with Protein A and Protein G beads for 6 hours. Chromatin isolated from 500 wild-type and 100 mutant imaginal discs were added to antibody coated beads and incubated overnight at 4 °C with end to end rotation in a 1ml volume. ChIP-nexus digestion and library preparation was performed as published (He et al., 2015), with the following modifications. To repair the DNA ends, NEB Next End Repair Module (NEB#E6050) was used, and reactions were set up in a 50µl volume at 20°C for 1h in thermomixer with gentle mixing. Beads were washed as described previously. The dA tailing reactions were set up in a 50µl final volume, incubated for 30 minutes at 37°C using the NEBNext dA-Tailing Module (NEB#E6053). The PCR amplification of nexus

library was performed using the NEB Next High-Fidelity 2X PCR Master Mix (NEB#M0541). All the samples were sequenced with Illumina NextSeq 500.

QUANTIFICATION AND STATISTICAL ANALYSIS

iRegulon Normalized Enrichment Scores (NES):

For a certain gene set as input, the enrichment for each motif (9713 unique PWMs) is determined by the Area Under the Recovery Curve (AUC) of the cumulative recovery curve, along the whole-genome ranking. A Normalized Enrichment Score (NES) is computed as the AUC value of the motif minus the mean of all AUCs for all motifs and divided by the standard deviation of all AUCs. This is very similar to a z-score, and a NES score of 3 corresponds to an FDR (false discovery rate) of 0.03 to 0.09. A high NES for a certain motif indicates that this motif is significantly overrepresented in the immediate regulatory space (5kb upstream and all introns) of the genes from the input set (Janky et al., 2014).

RNA-seq analysis

Raw reads were cleaned for adapter sequences using *fastq-mcf*. Cleaned reads were mapped on *Drosophila melanogaster* FlyBase release r6.03 using TopHat2 (Kim et al., 2013) (Bowtie2/2.2.1-intel-2014a). Htseq-count (Anders et al., 2015) (HTSeq/0.6.1p1-foss-2014a-Python-2.7.6) was used to assign reads to genes using the *dmel-all-r6.03.gff* template. The raw counts matrix (6 conditions each with 3 biological replicates) was further processed and size factor was normalized in R. The list of 350 upregulated genes in *cic wts* double mutants vs wild type controls was obtained using DESeq2 (Love et al., 2014) (differential analysis with 3 replicates, cutoff; average expression > 50, logFC > 0.5 and adjusted P-value < 0.01). These 350 genes were subdivided into four groups, based on their normalized expression values (log₂ transformed) in the *day_5* samples, using an unsupervised clustering method (Self Organizing Tree Algorithm, standard parameters in MeV) (Saeed et al., 2003). Genes from *wts* cluster whose expression increased more than 1.3 folds from *wts* to *cic wts* were added to the synergistic cluster. The final set of 46 synergistic genes was obtained by filtering out genes whose expression dropped below wild type levels in *cic wts day_9*. Motif enrichment analysis was carried out on each gene set using iRegulon v1.4 (Janky et al., 2014), (plugin for Cytoscape) using a library of 9713 PWMs, taking the full transcript and 5kb upstream of each gene into account. Expression heat-maps were generated with the NMF package in R (Gaujoux and Seoighe, 2010), using log₂ normalized counts and these options: `scale="row", Rowv=F ,Colv=NA, annRow=medianexp`.

ChIP-nexus analysis

Mapped bam files and bigwig files were generated as described from the sequenced reads (He et al., 2015). Scaloped peaks were called on the (unclipped) mapped reads, using the MACS2 software suite (Feng et al., 2011) (`macs2 callpeak -t sd_genotype.bam -g dm -n sd_genotype.macs2 --keep-dup all --call-summits`). ChIP peaks with sufficient reads (fold change > 10) were retained for further analysis. Cic peaks were called on the (unclipped) mapped reads, using Cic-ChIP in *cic wts* mutants samples as control (`macs2 callpeak -t cic_genotype.bam -g dm -n cic_genotype.macs2 --bdg --nomodel -c cic_cic.wts.bam`). Using the negative controls (Cic pulldown in *cic wts* discs) removed most of the noise, allowing us to use all the called peaks for further analysis. The retained ChIP peaks were used as input sets for i-cisTarget (Imrichová et al., 2015), a tool that identifies significantly enriched motifs in a set of (ChIP) regions. Directly bound regions were defined as those regions that had their respective transcription factor DNA binding motifs significantly enriched.

DATA AND SOFTWARE AVAILABILITY

RNA-seq and ChIP-nexus datasets have been deposited to NCBI's Gene Expression Omnibus. They are accessible through GEO Series accession number GSE96868.

ADDITIONAL RESOURCES

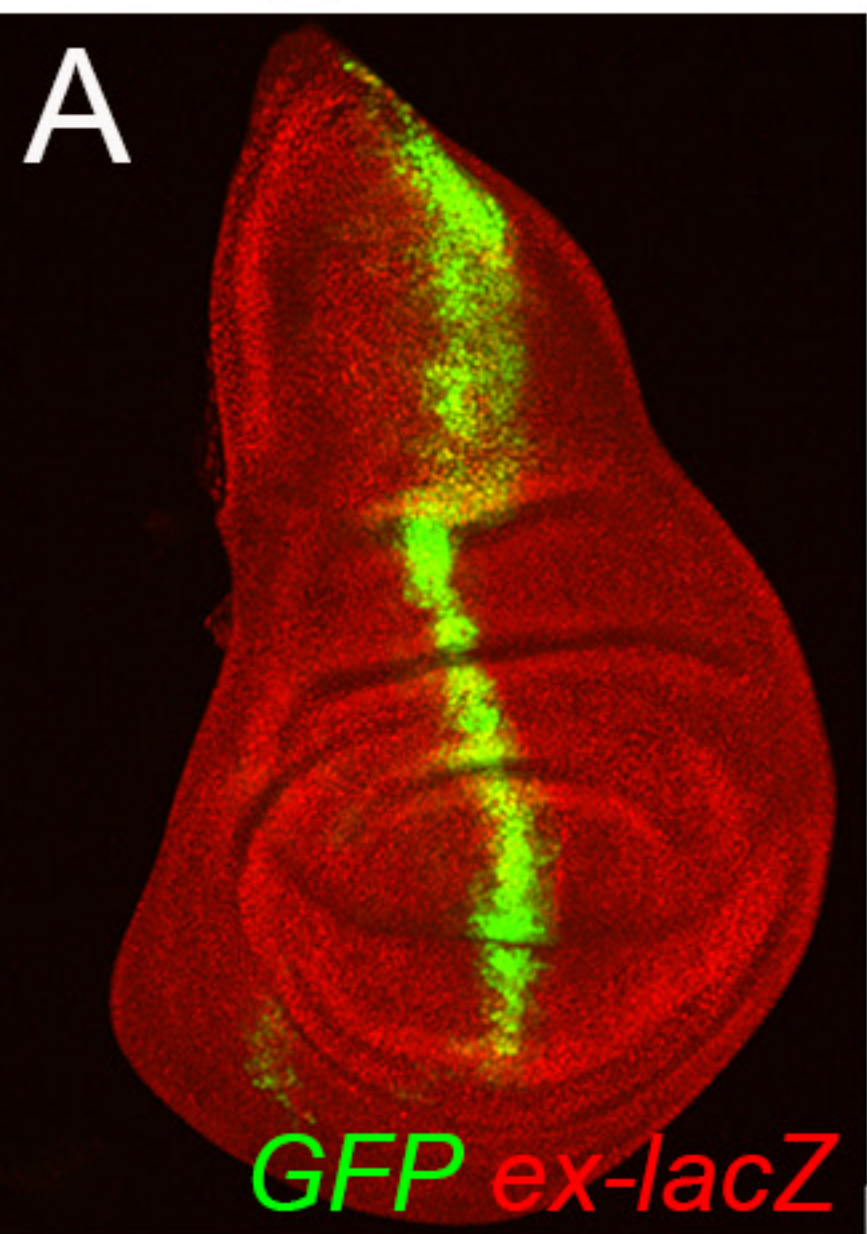
iRegulon: <http://iregulon.aertslab.org>

i-cisTarget: <https://gbiomed.kuleuven.be/apps/lcb/i-cisTarget/>

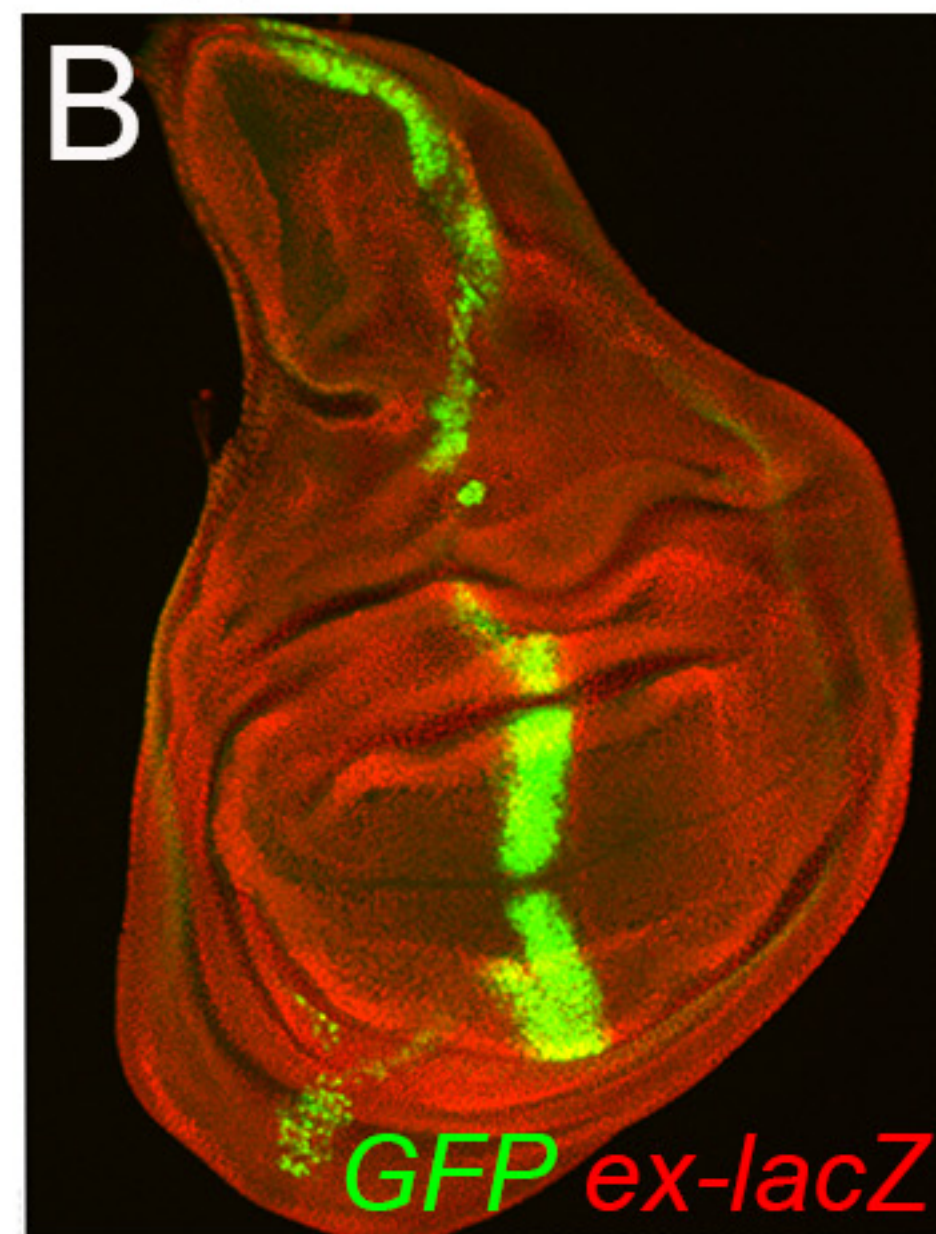
ChIP-nexus Protocol:
http://research.stowers.org/zeitlingerlab/documents/150709ChIP-nexusProtocol_000.pdf

Figure 1

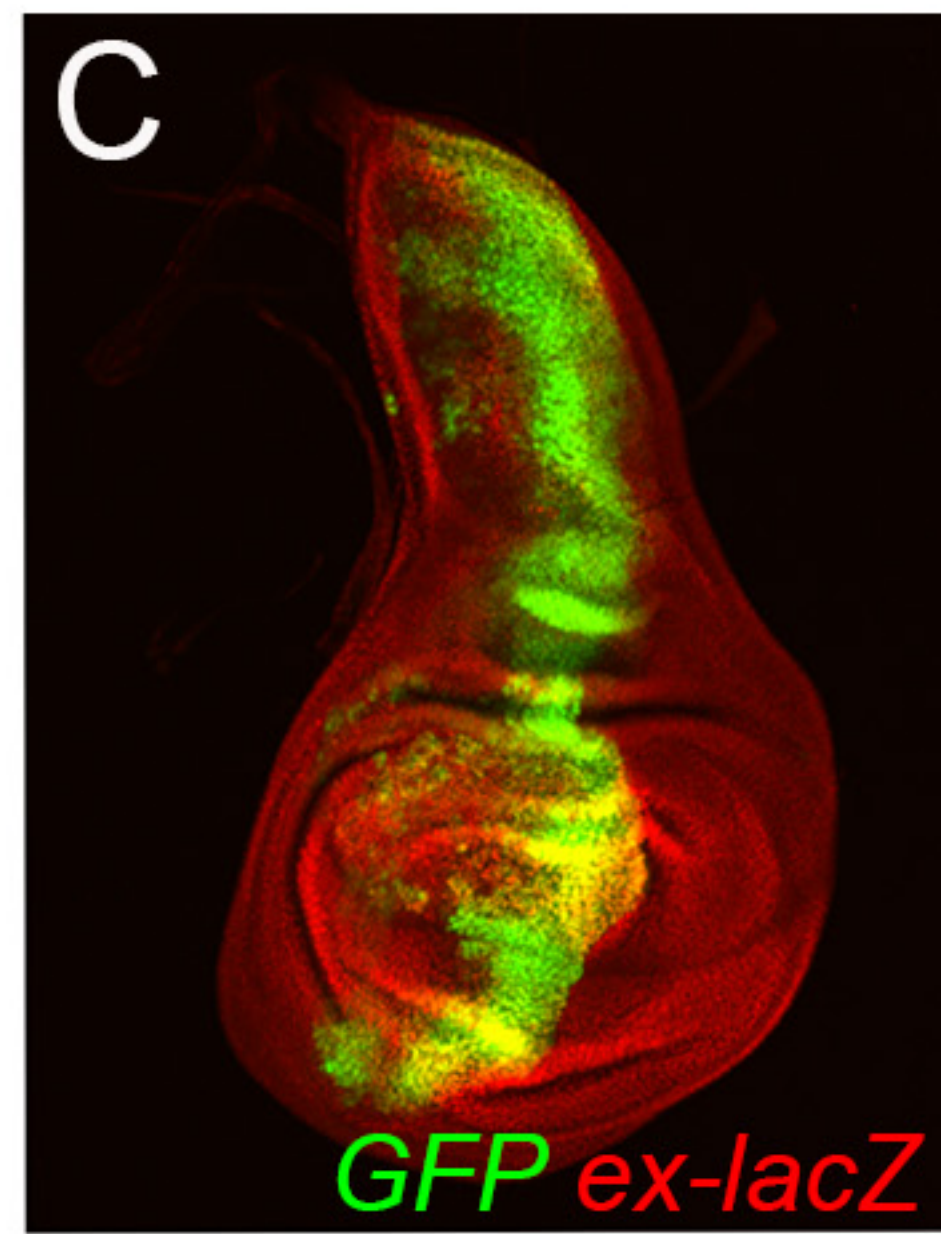
dpp > *GFP*



dpp > *GFP in ex*



dpp > *EGFR^{top}*



dpp > *EGFR^{top} in ex*

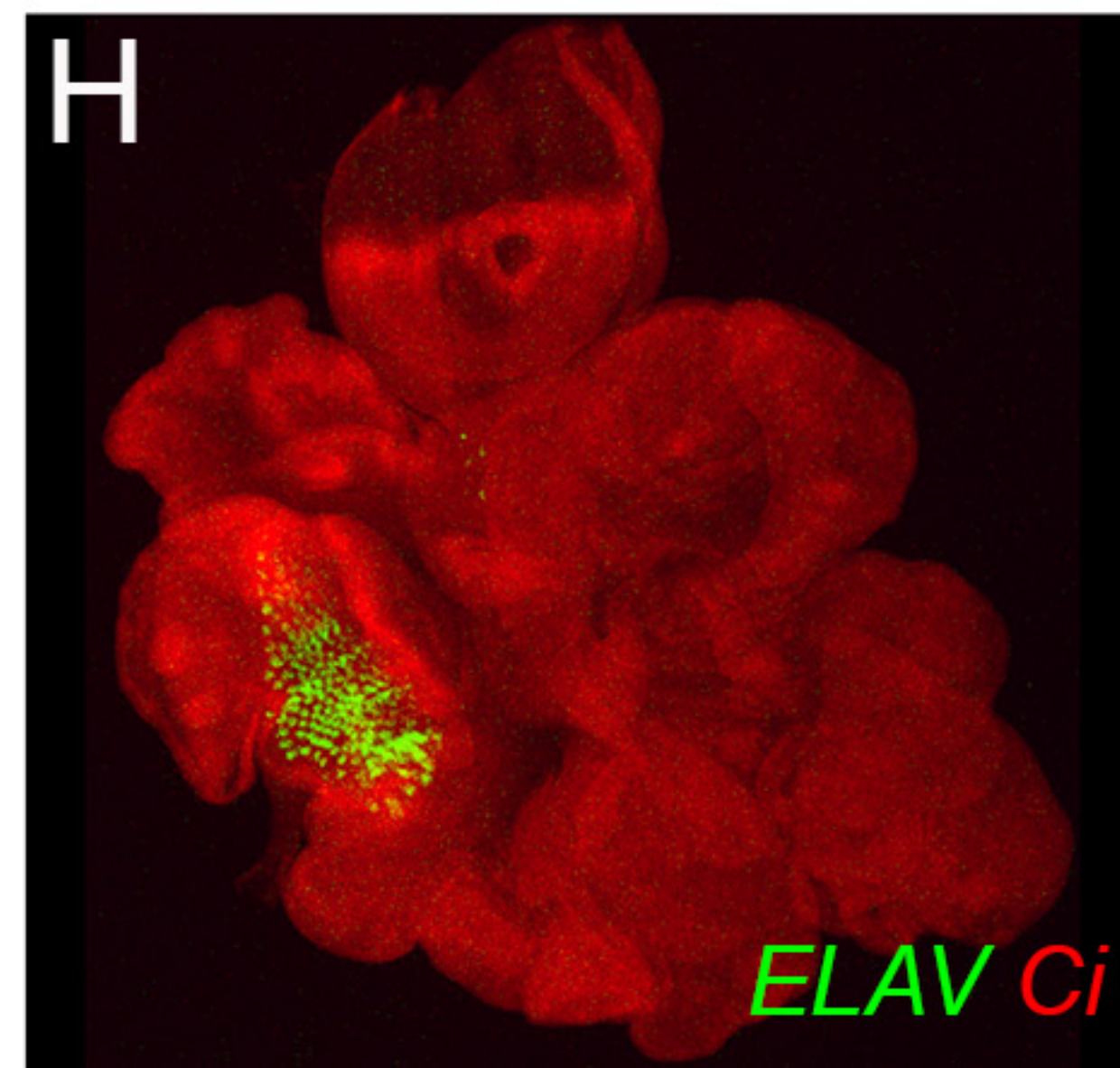
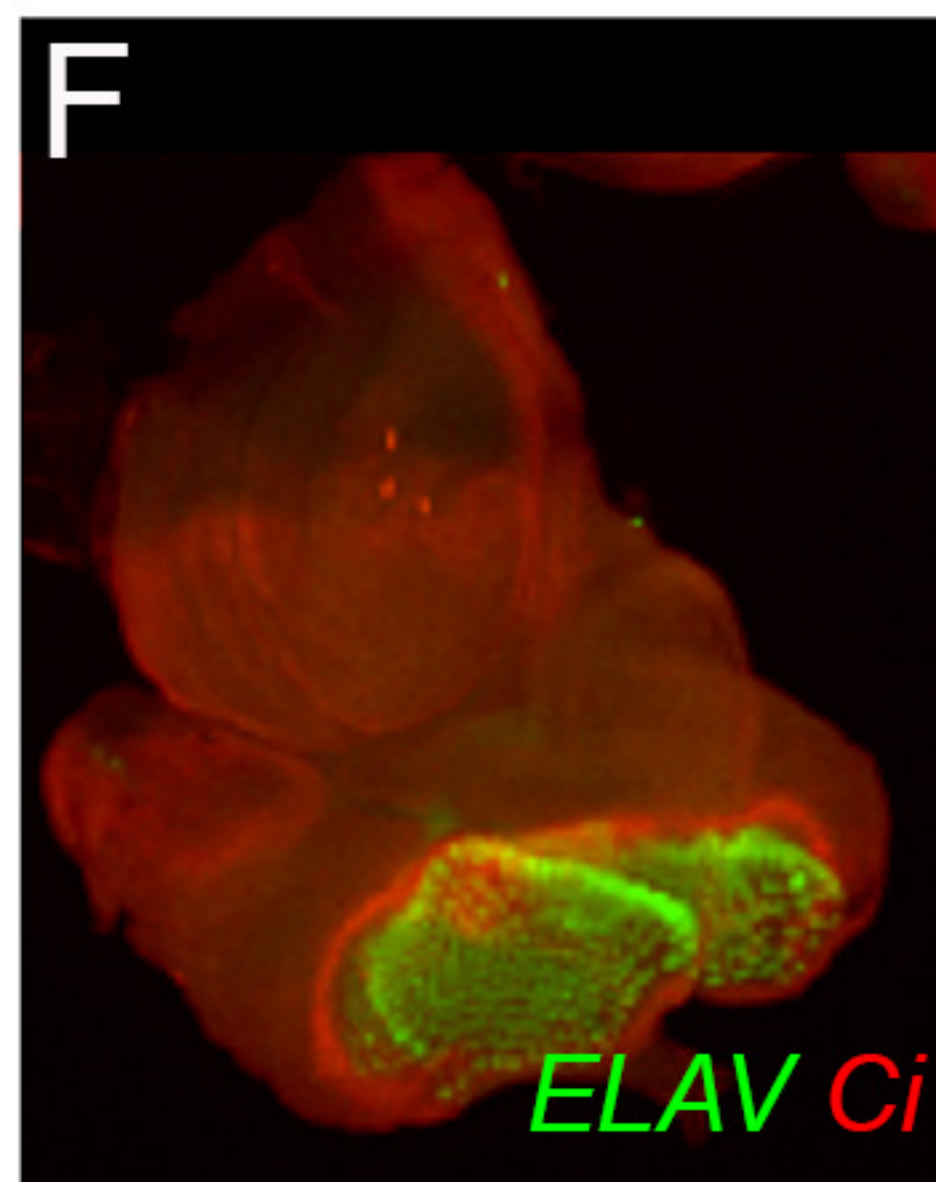
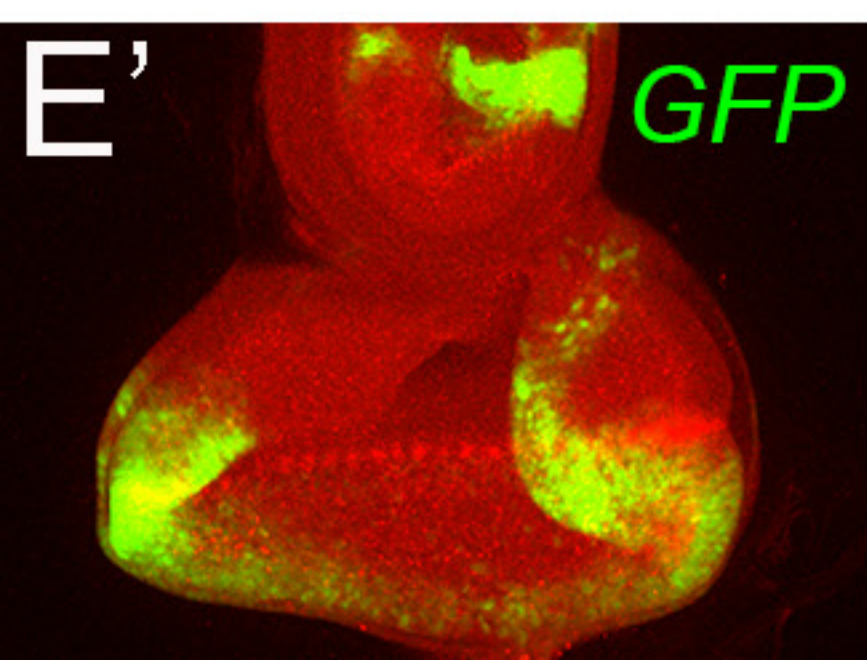
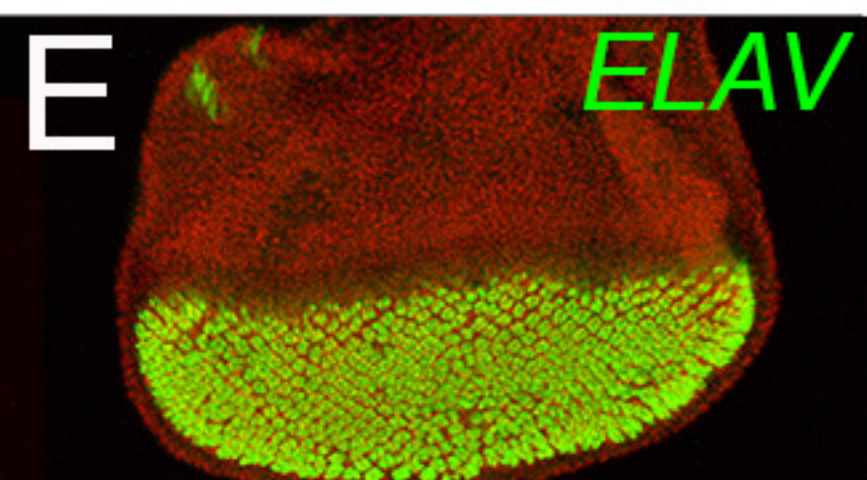
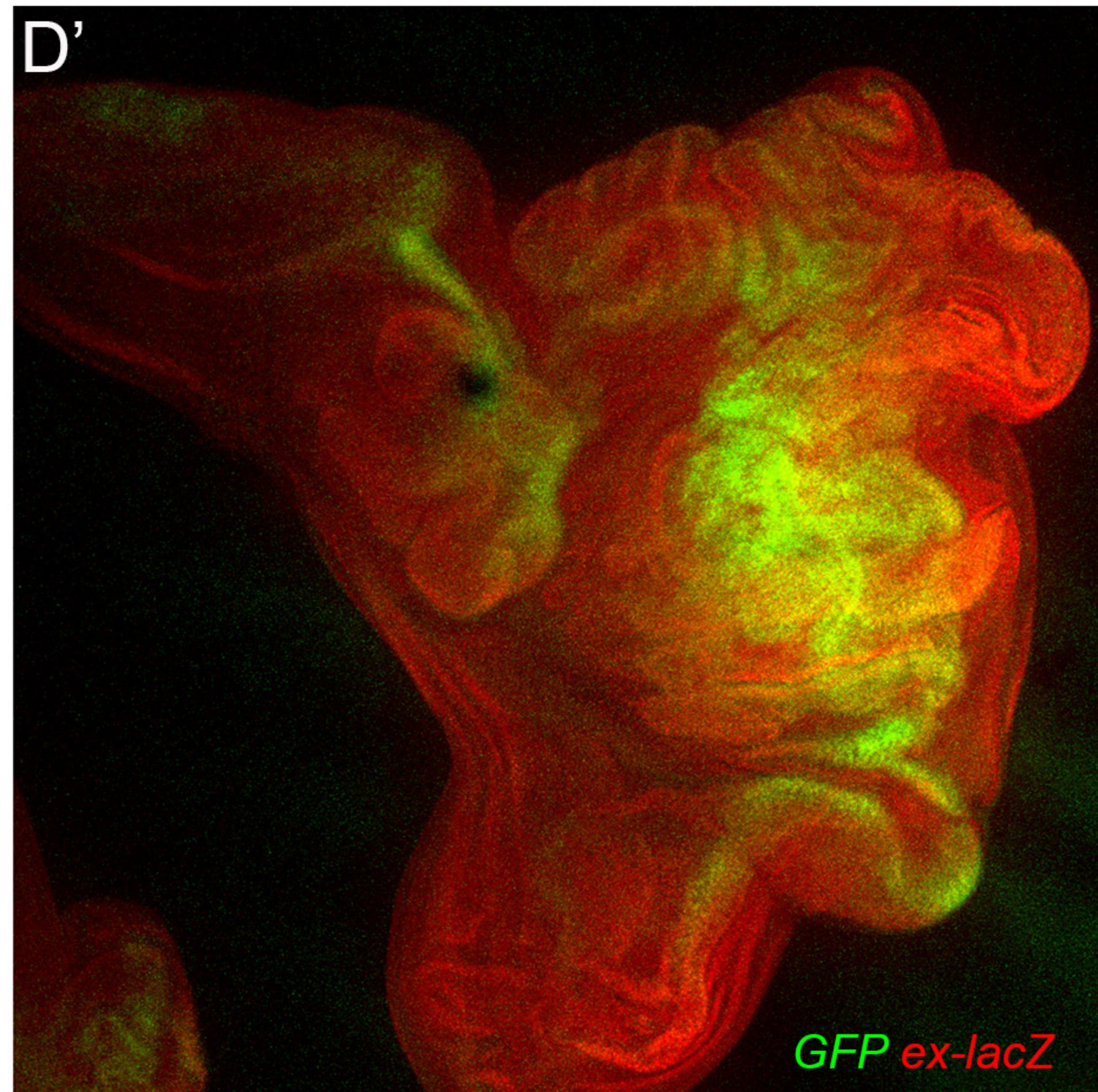
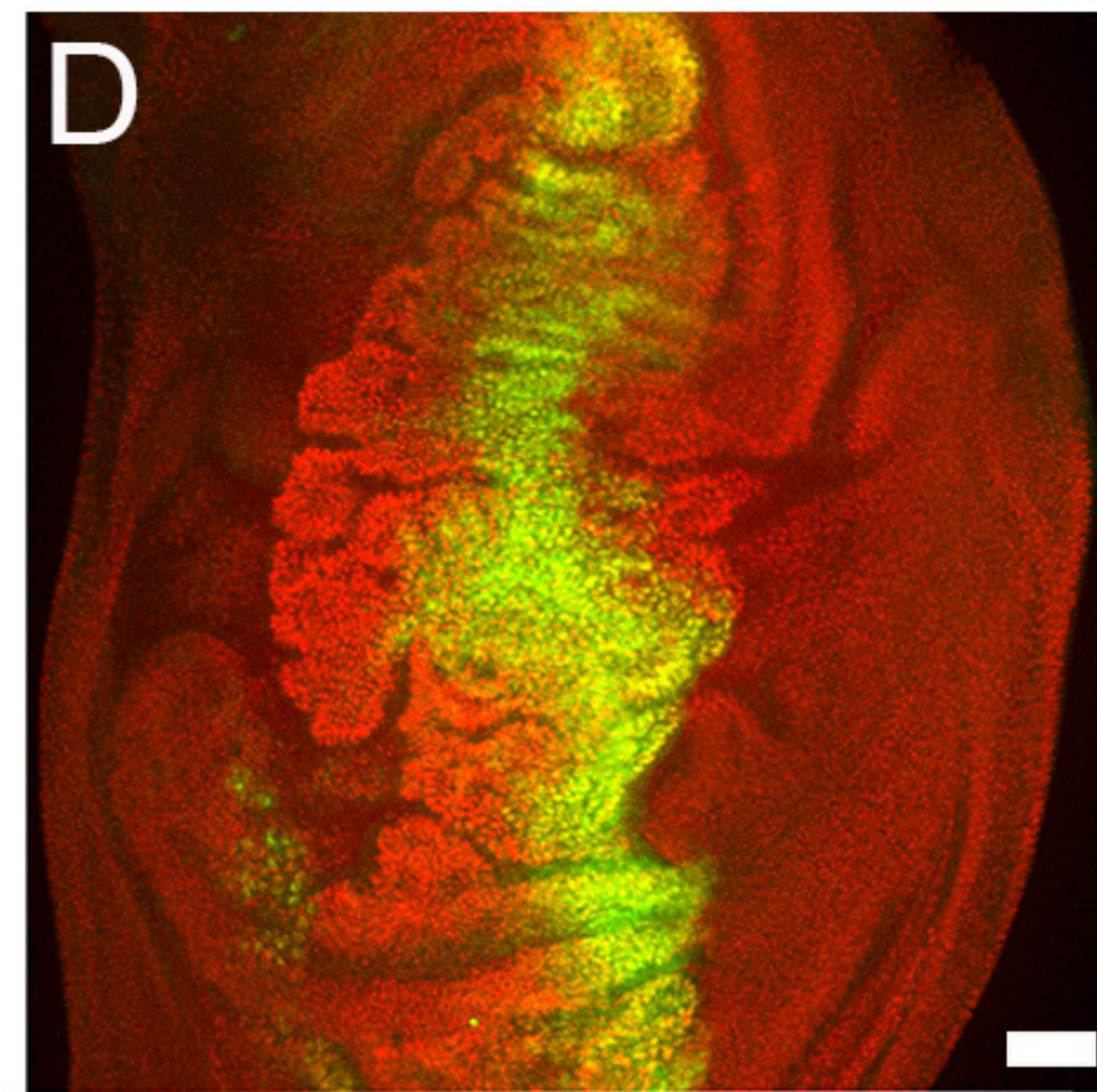
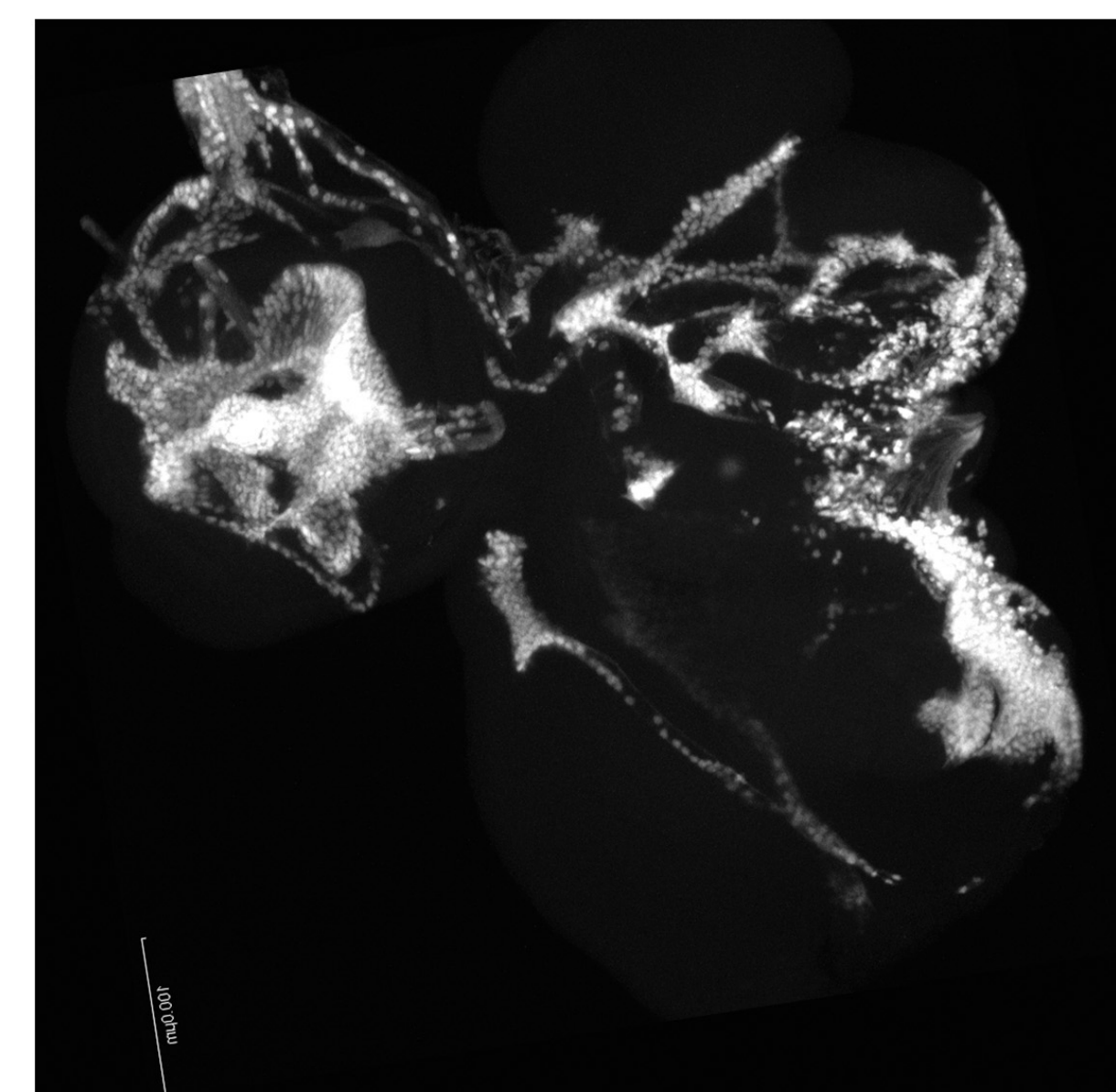
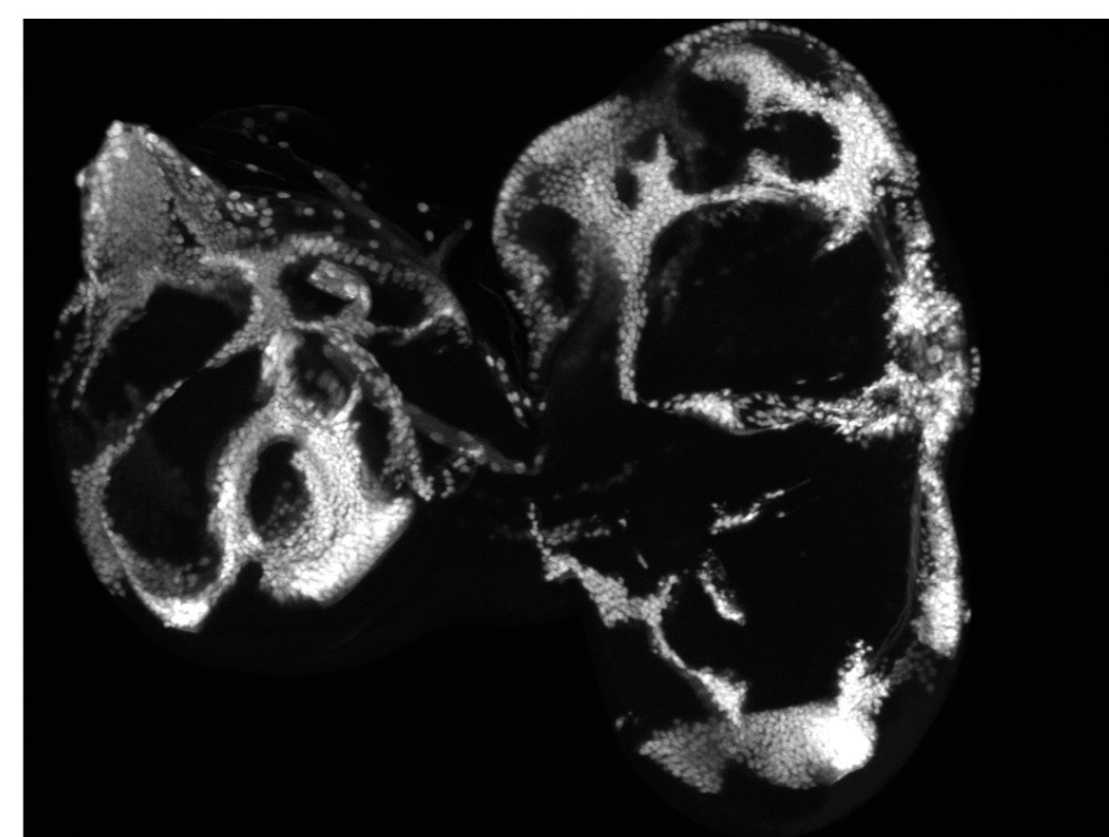
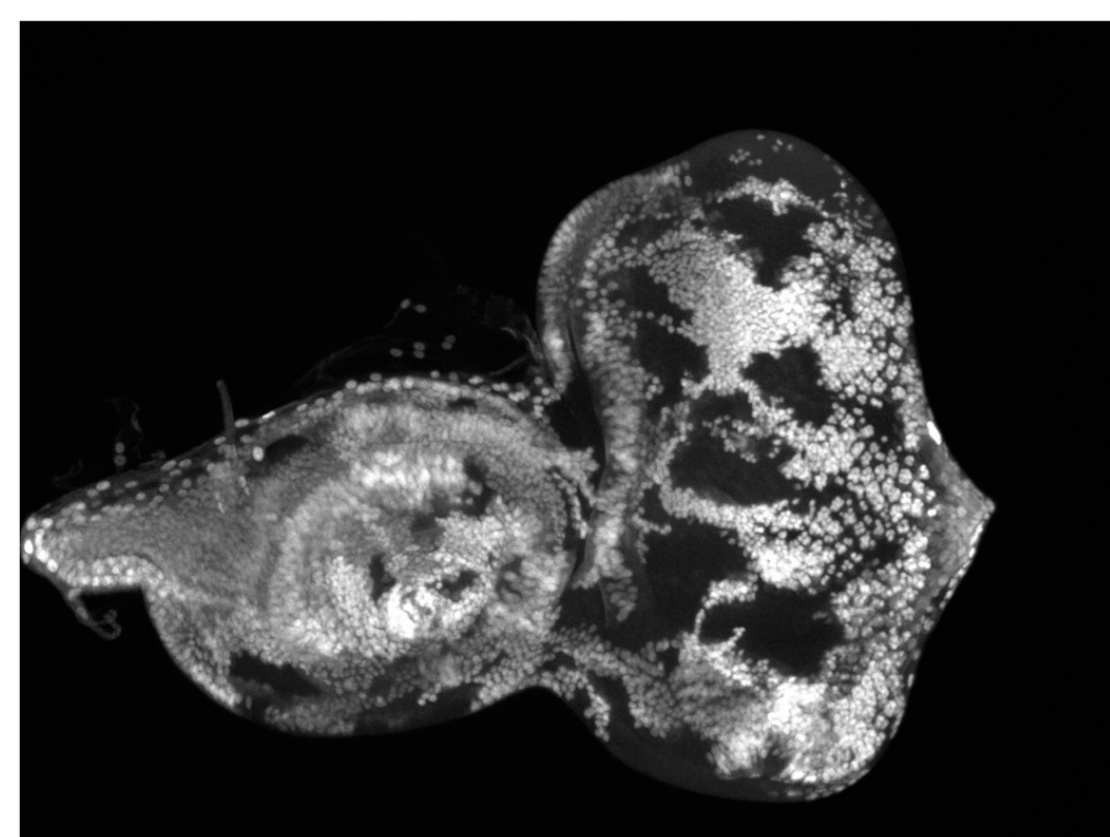
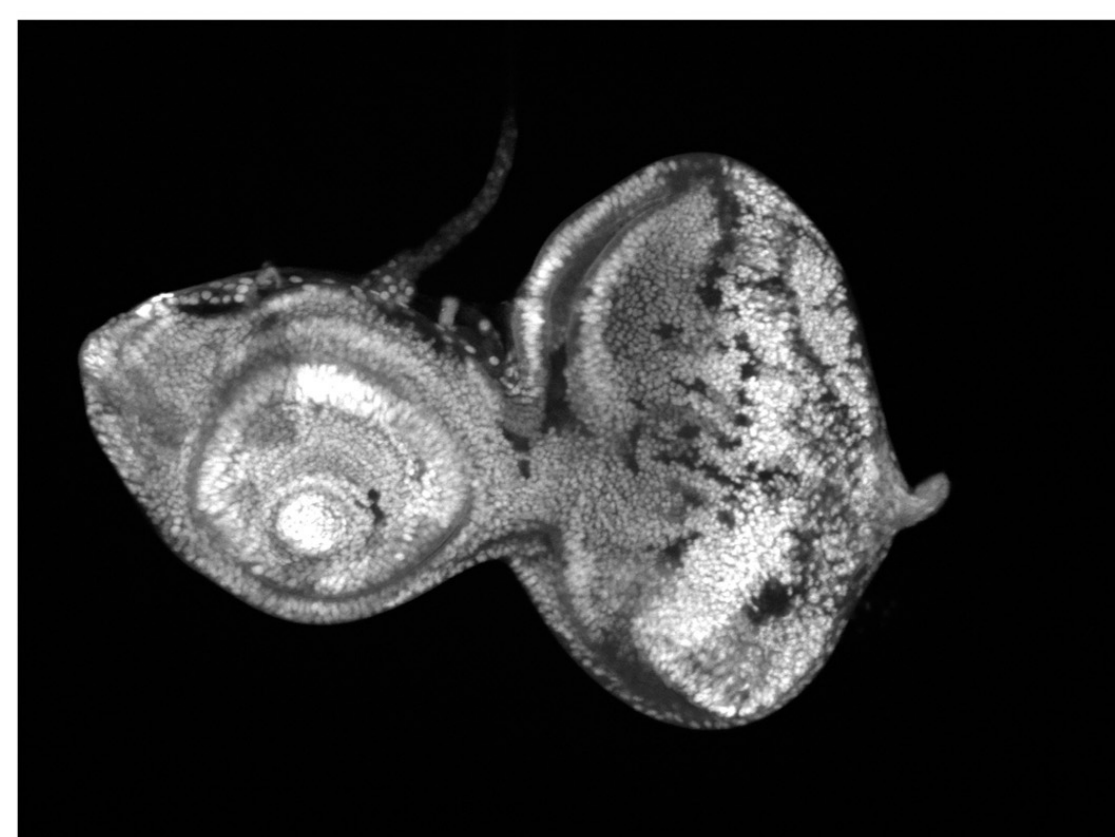
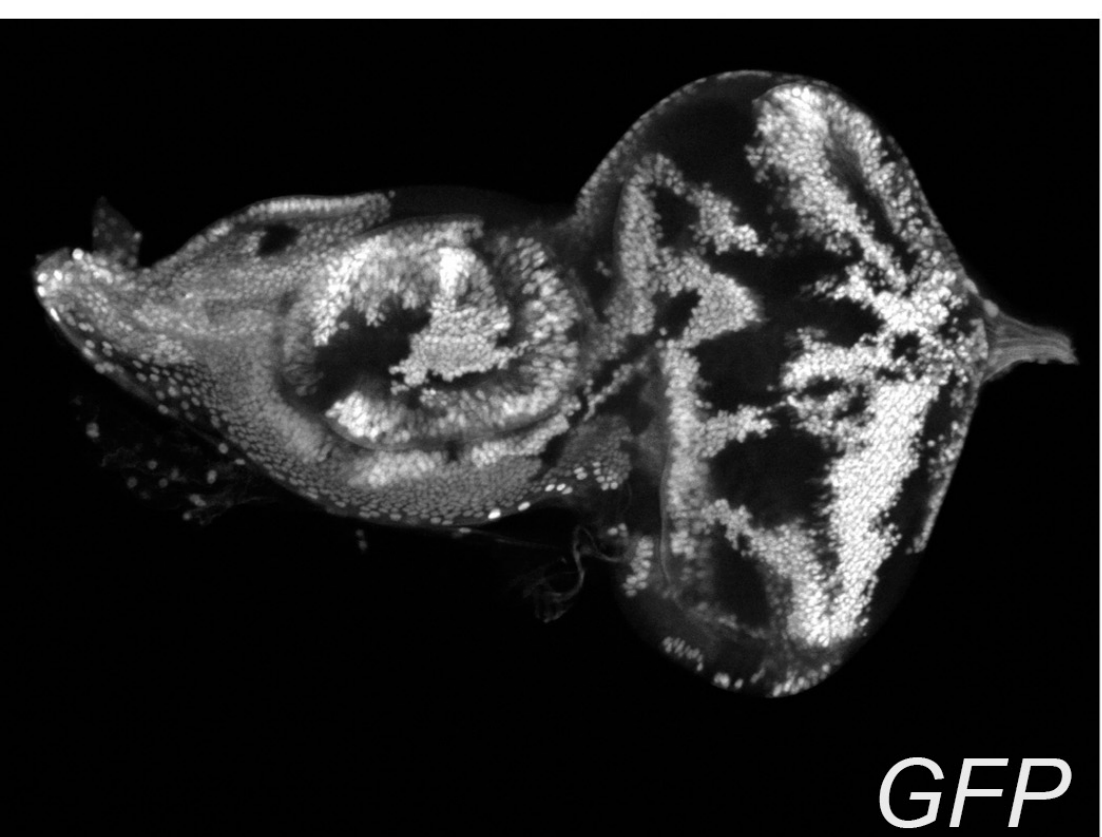
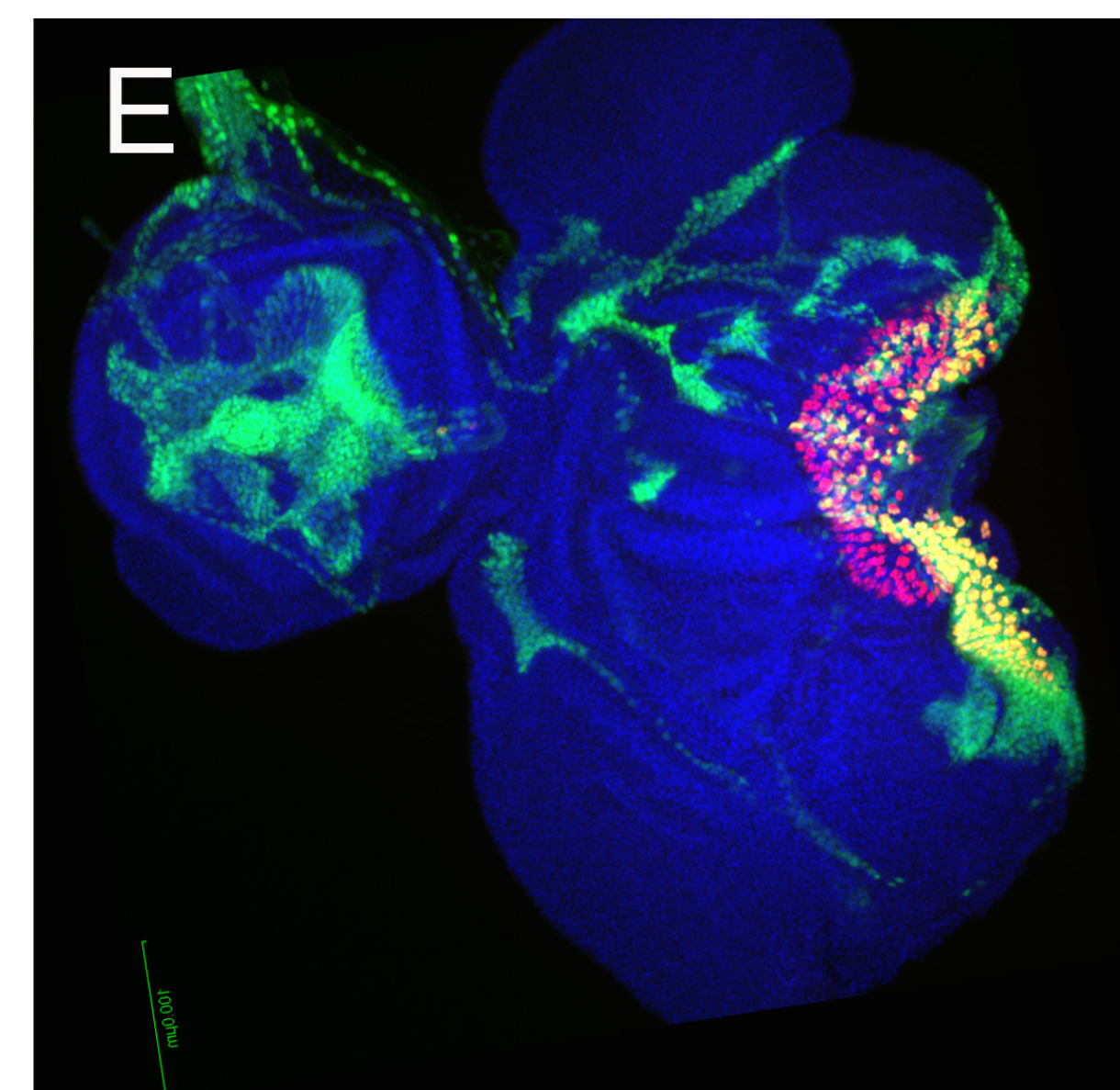
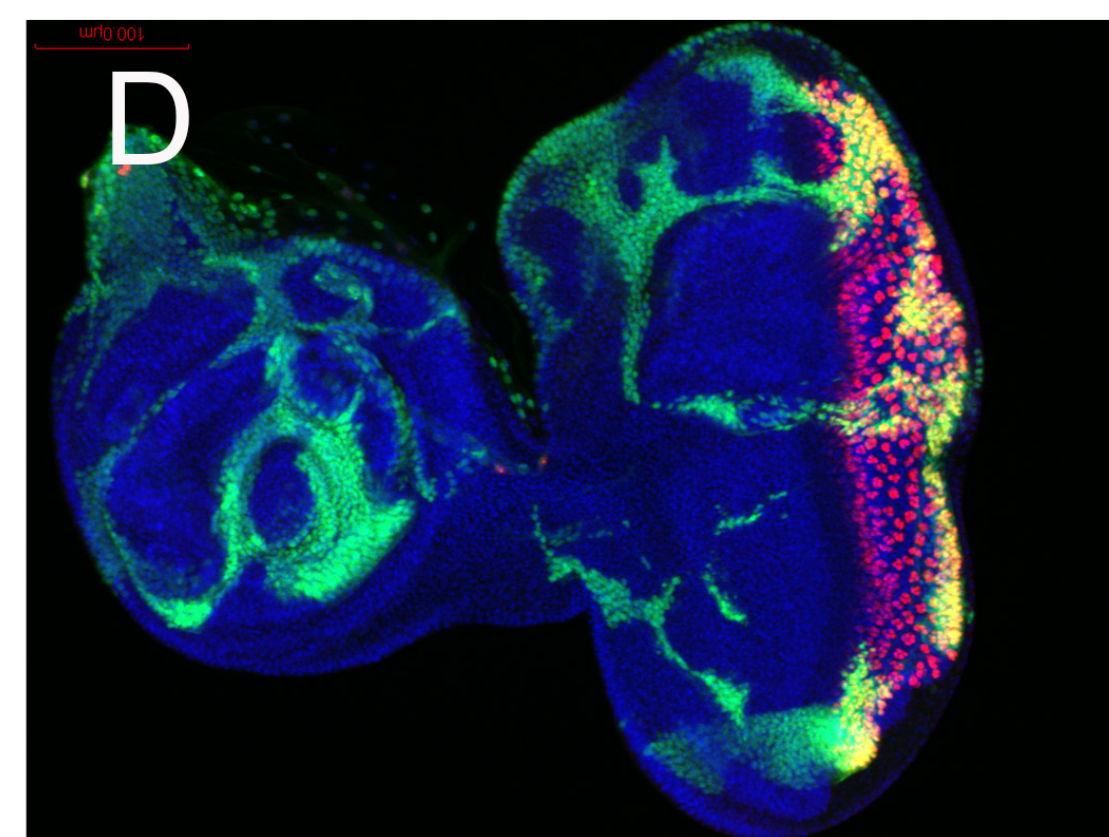
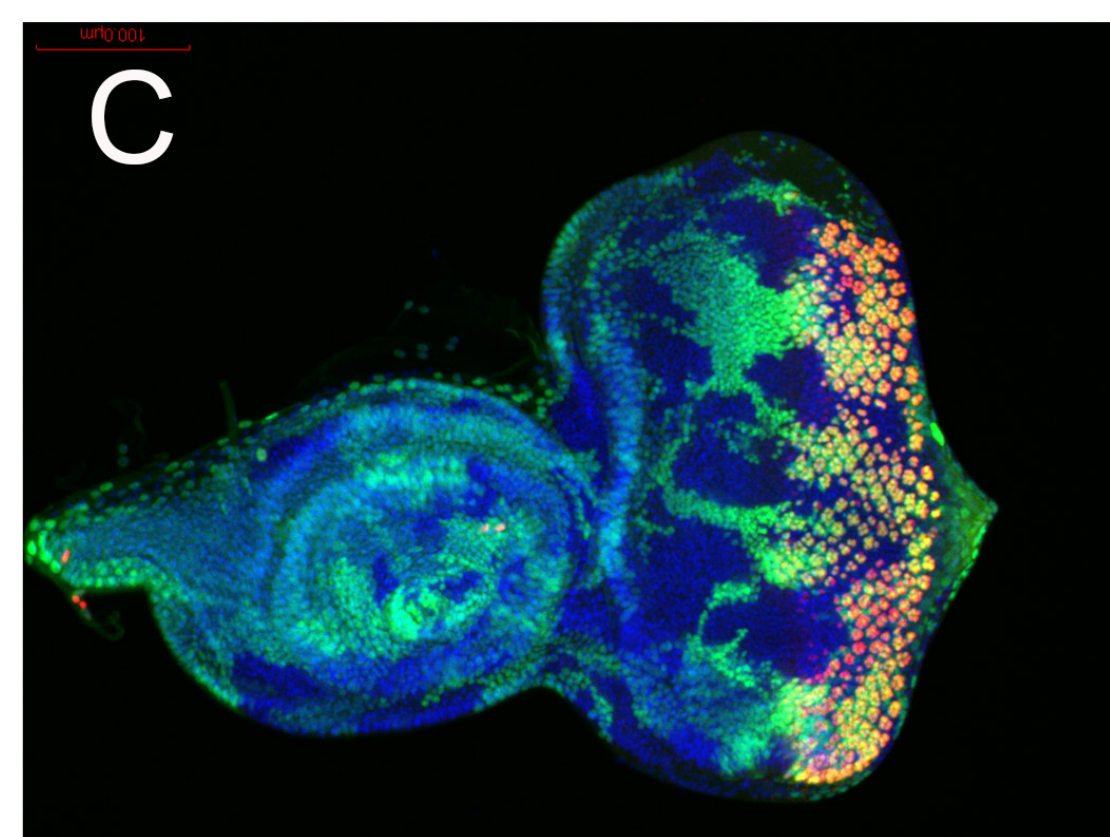
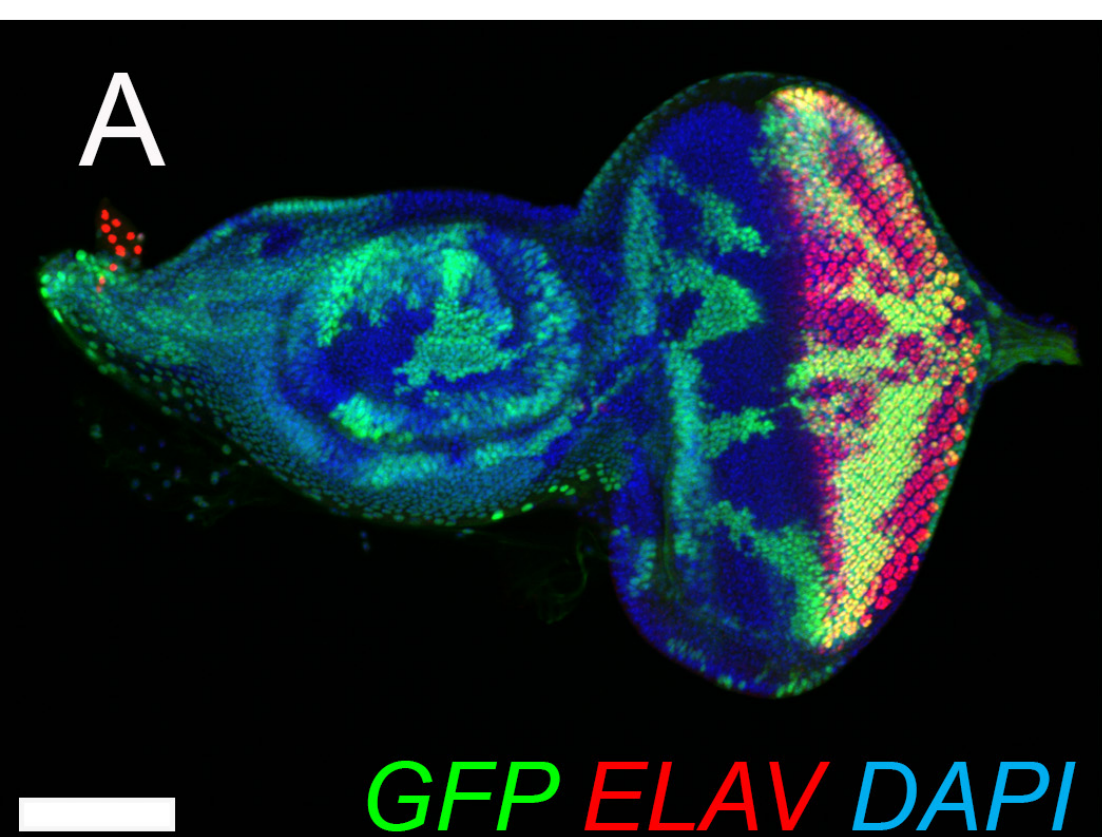


Figure 2



eyflp cic^{Q474X}



eyflp ras^{DC408}



eyflp ras^{DC408} cic^{Q474X}



eyflp wts¹⁴⁹

no adults

eyflp cic^{Q474X} wts¹⁴⁹

Figure 3

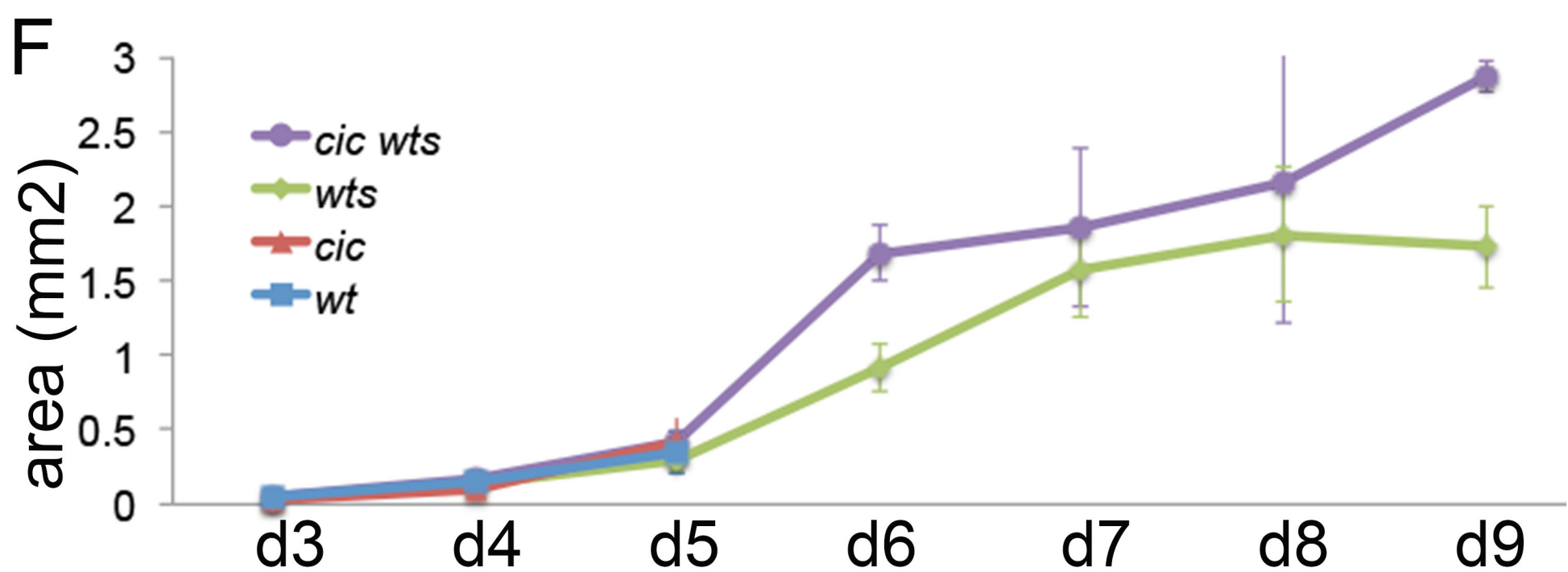
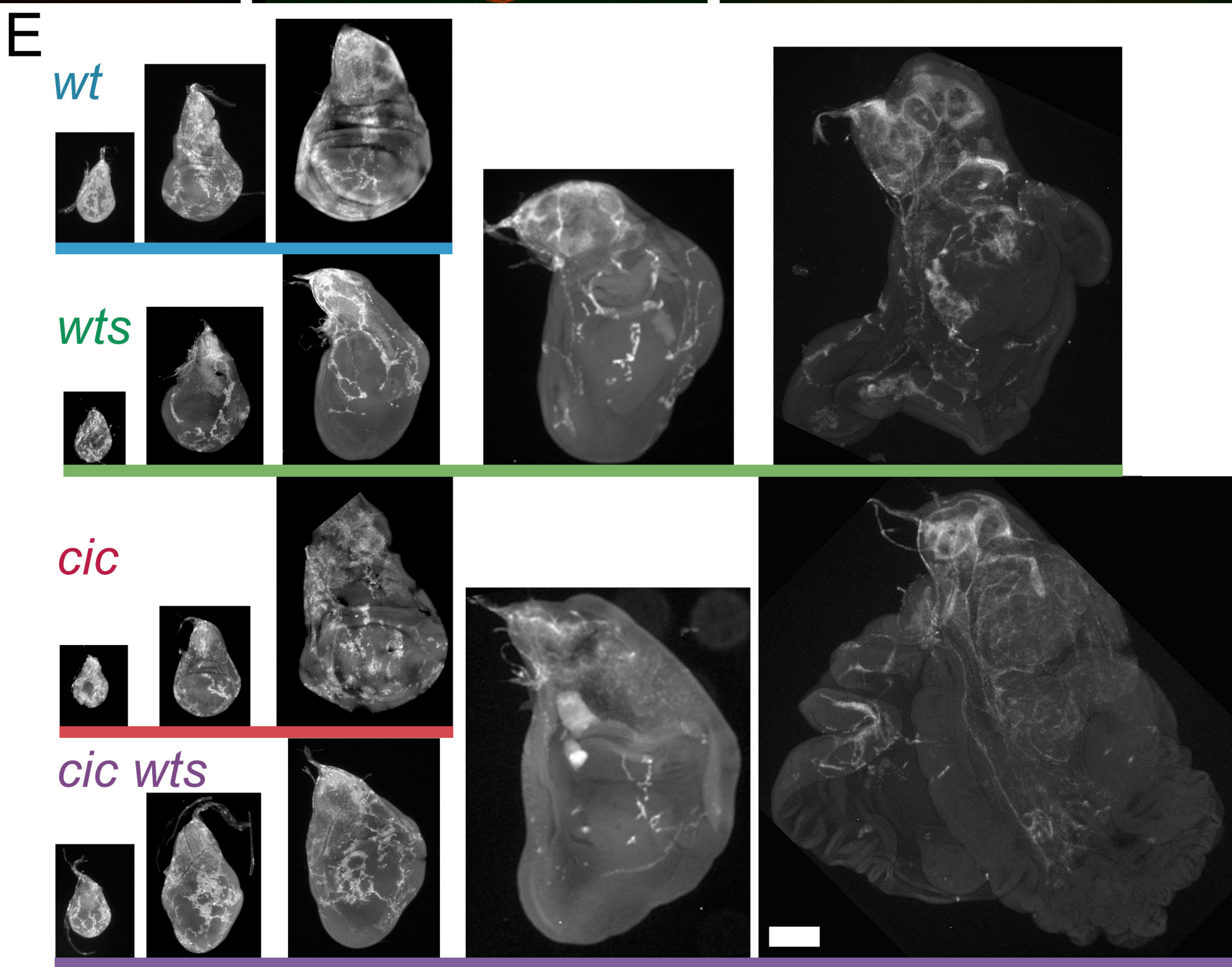
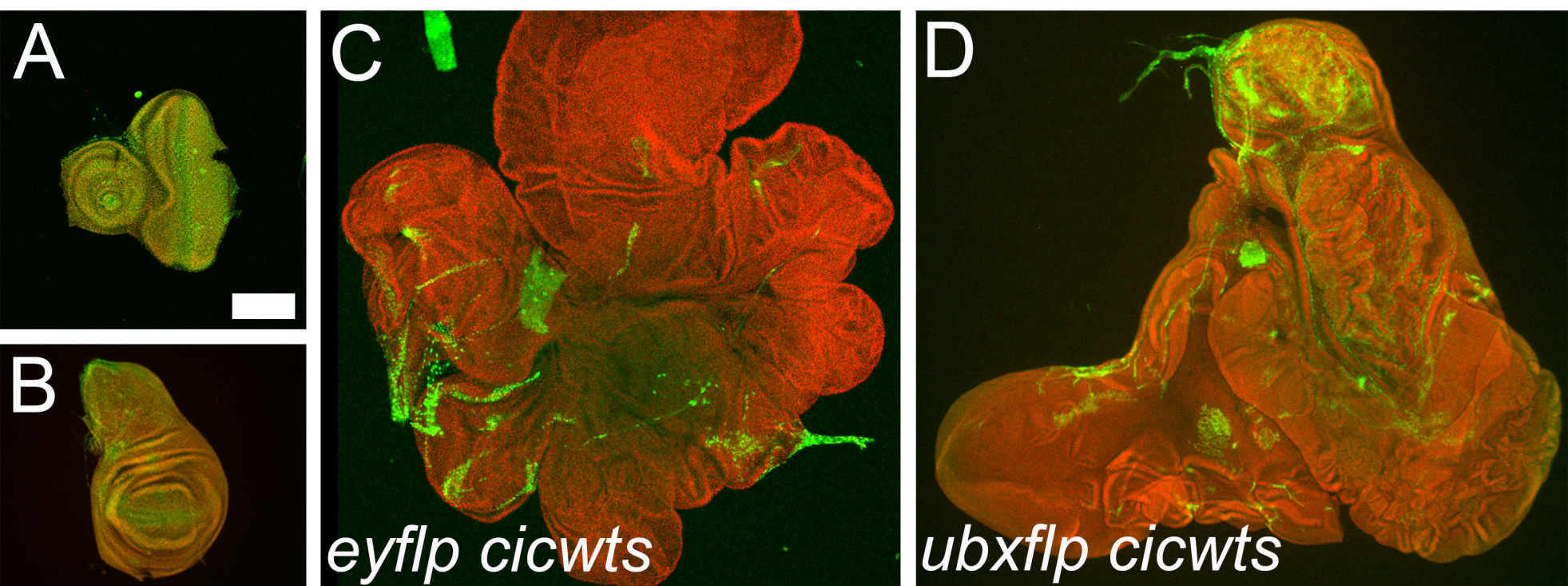
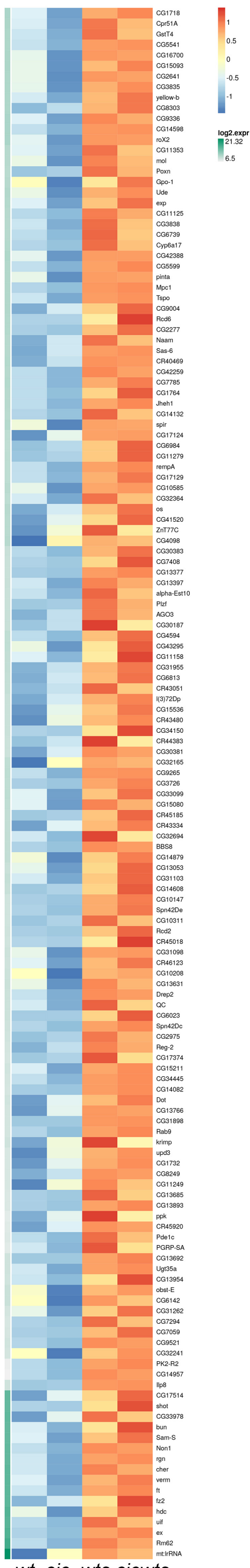
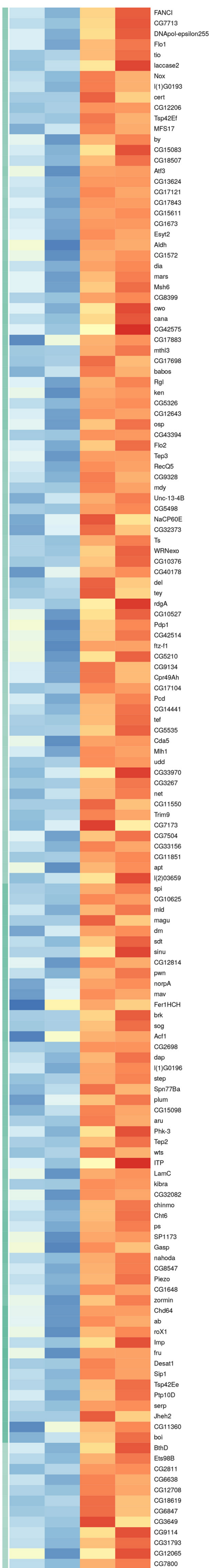
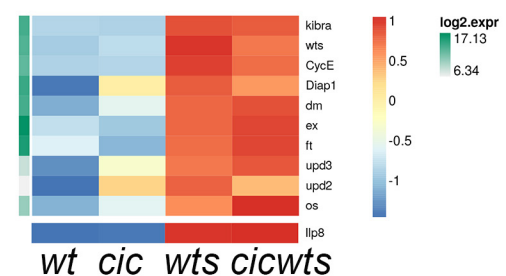


Figure 4

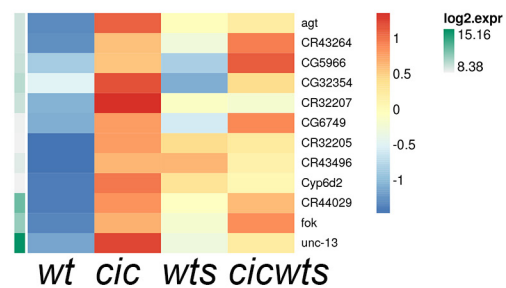
A Wts cluster



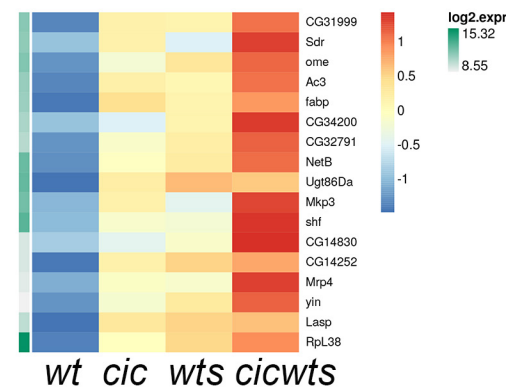
B Yki targets



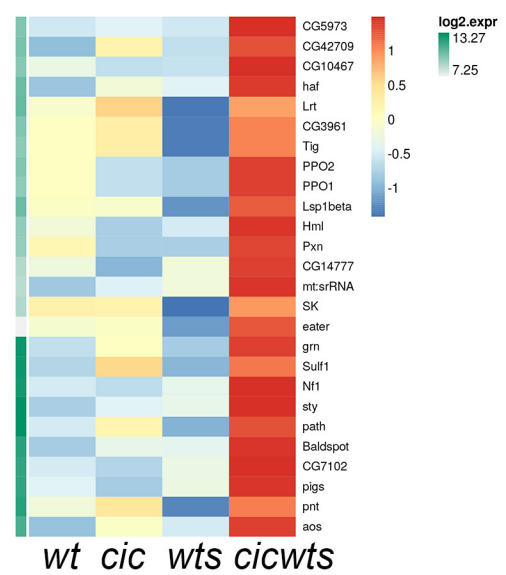
C Cic cluster



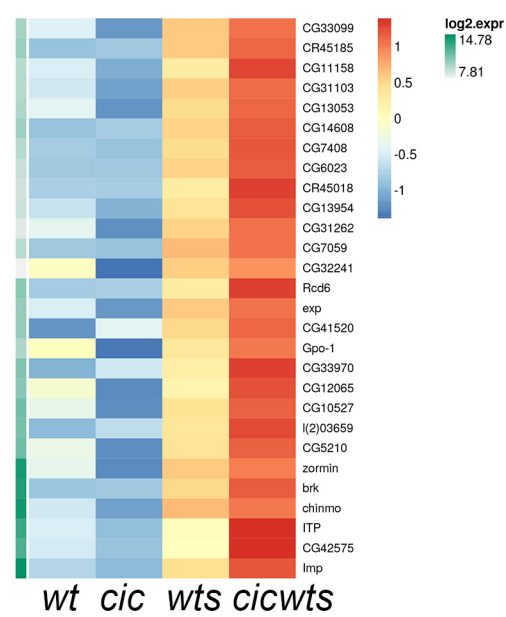
D Additive cluster

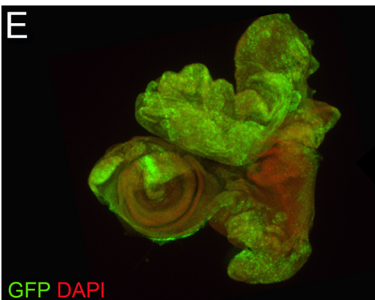
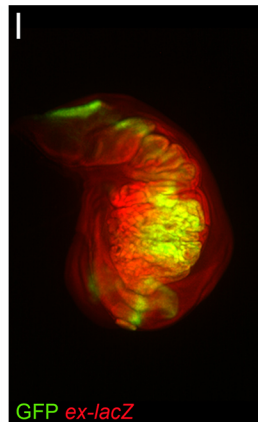
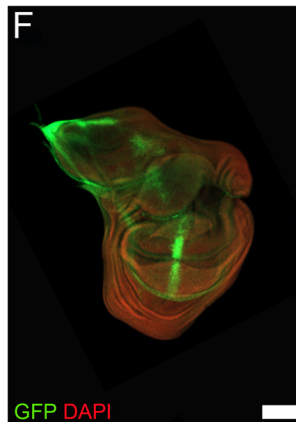
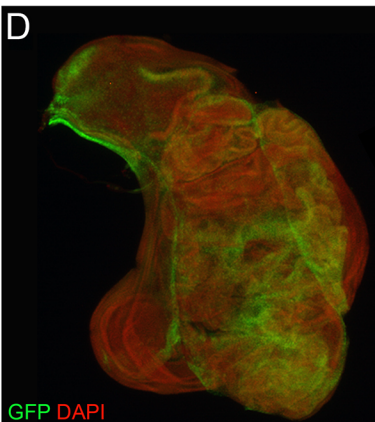
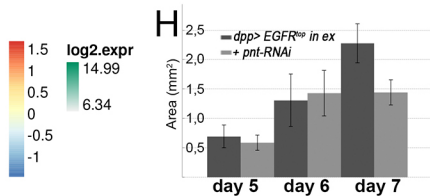
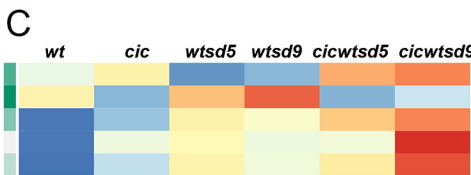
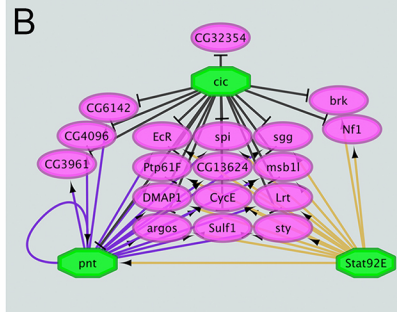
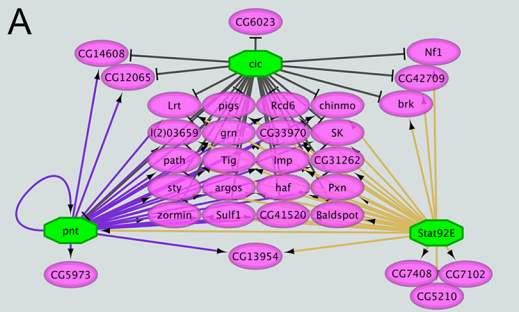


E synergistic cluster

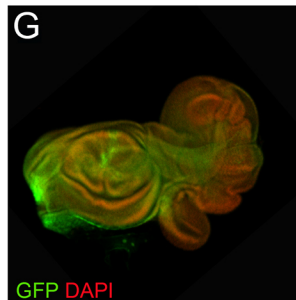


F from Wts cluster

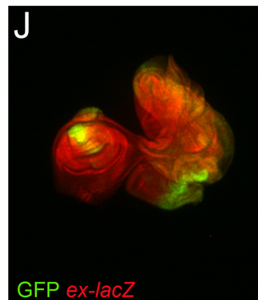




dpp > EGFR^{top} in ex



dpp > EGFR^{top} + Socs36E in ex



dpp > EGFR^{top} + pnt-RNAi in ex

Figure 6

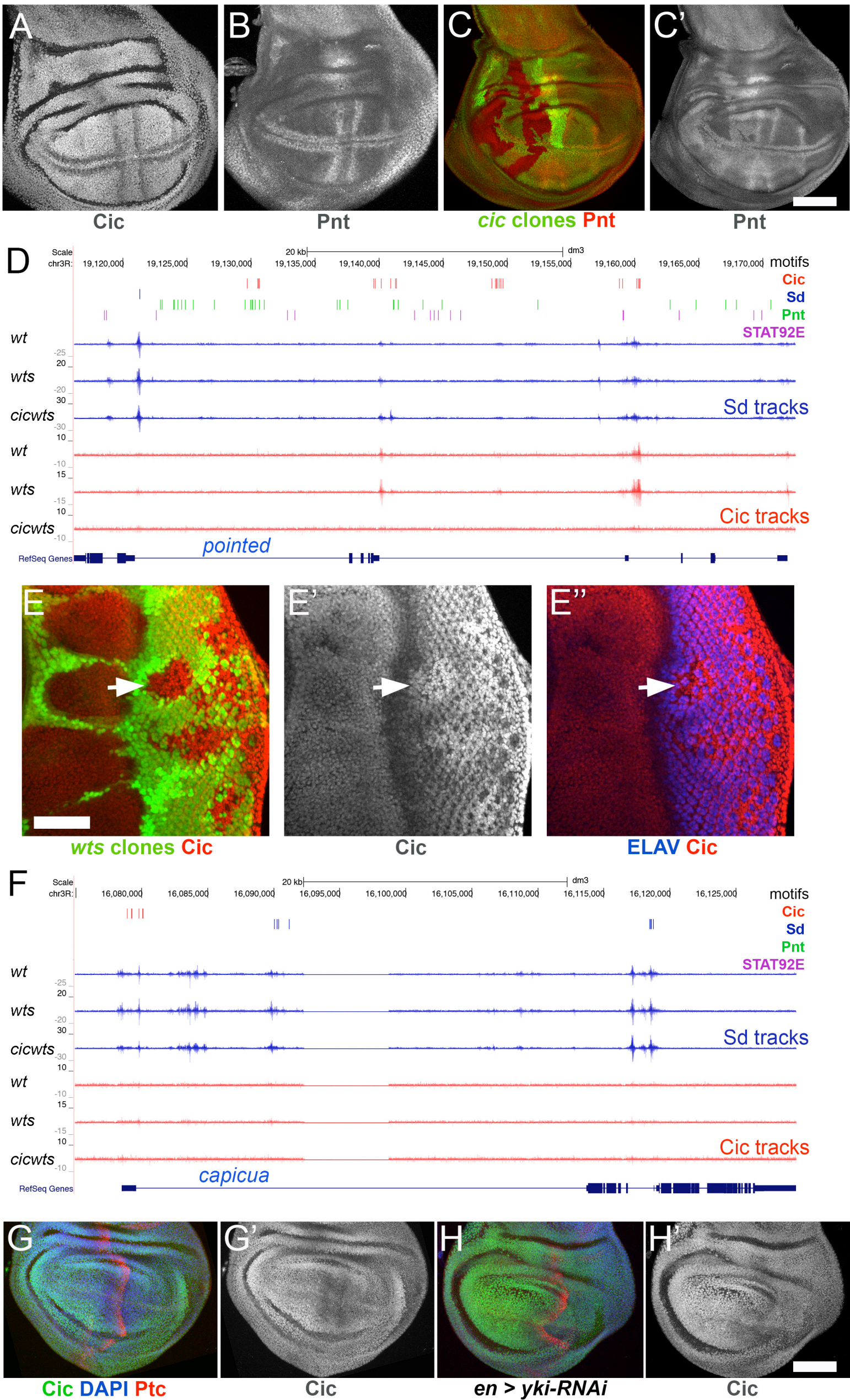
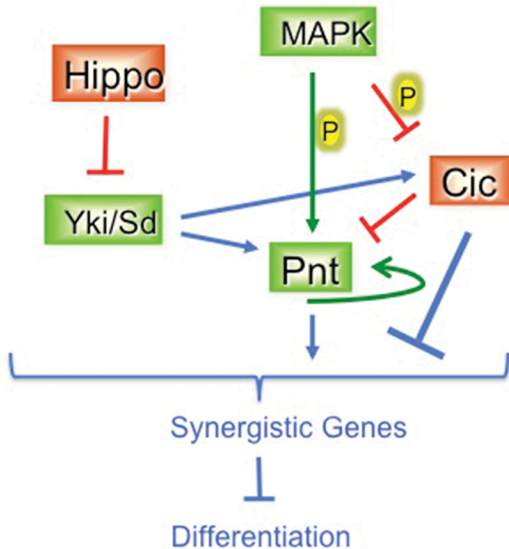
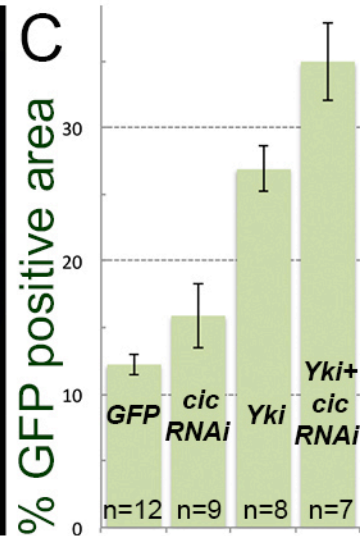
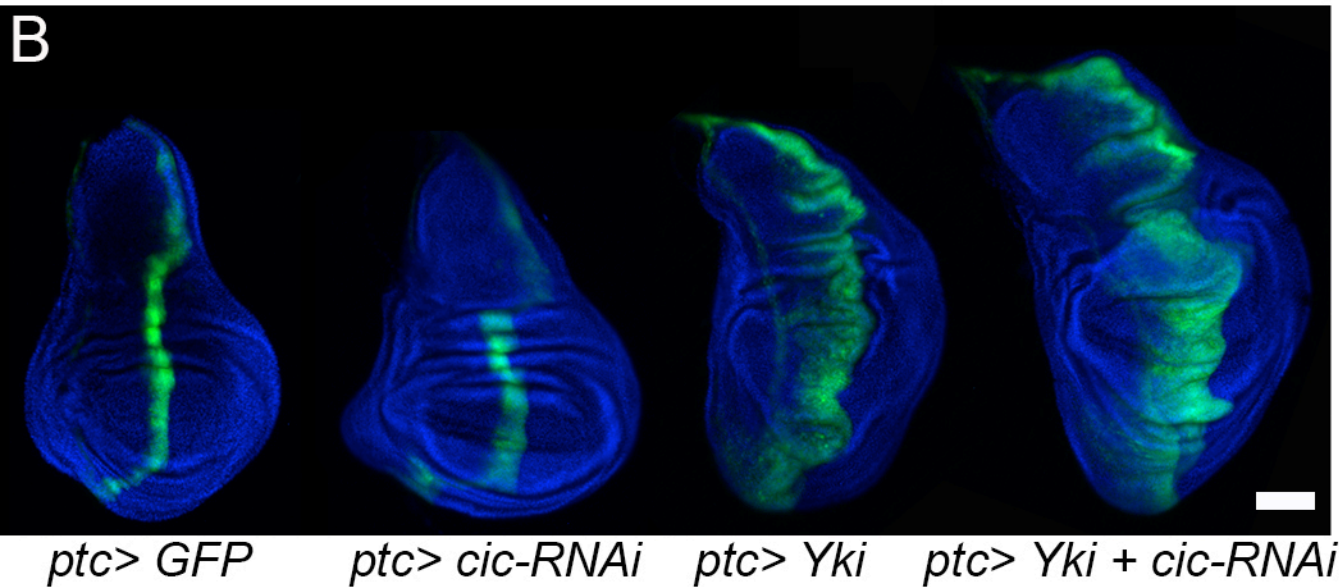
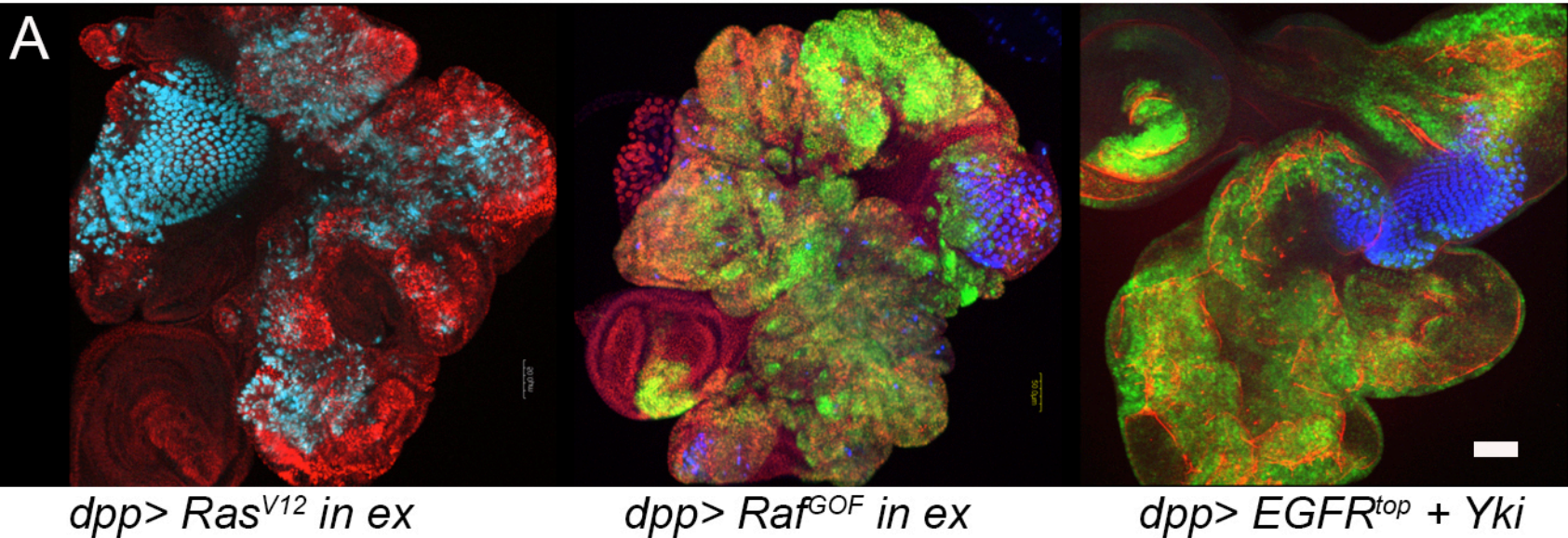


Figure 7

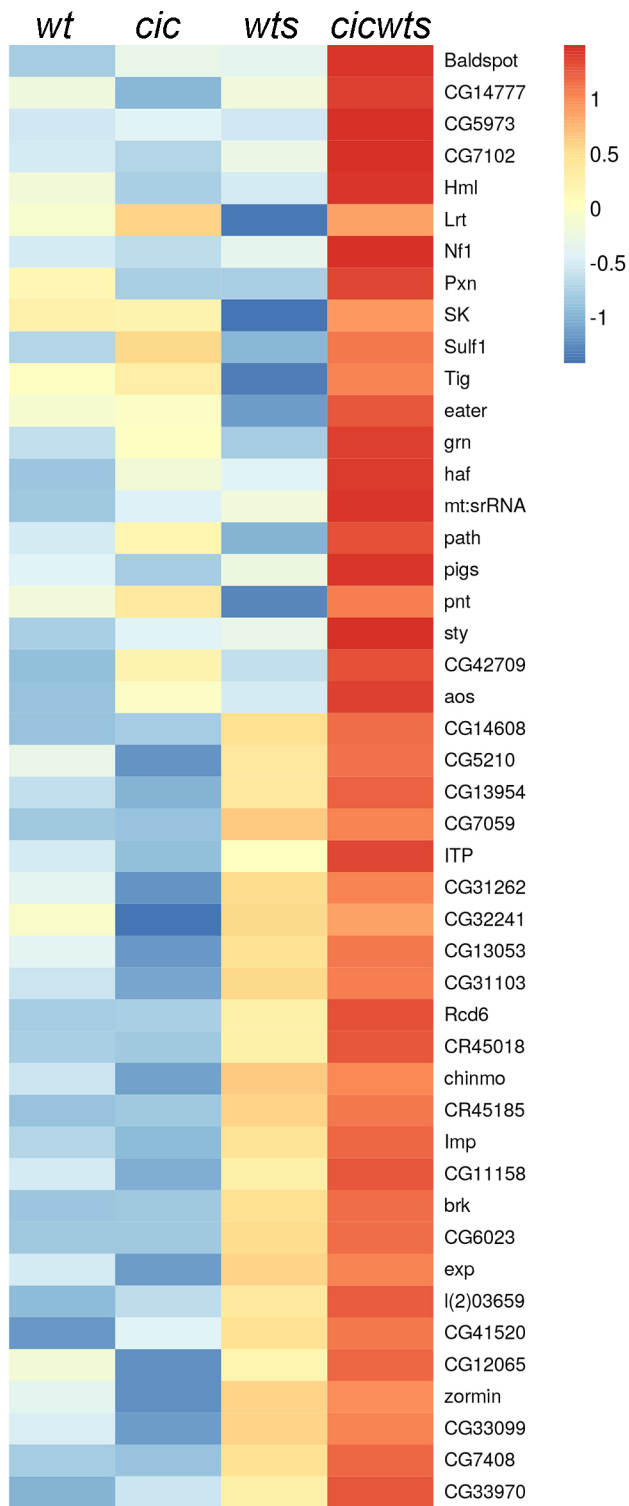
Hippo and Cic provide breaks that prevent transformation



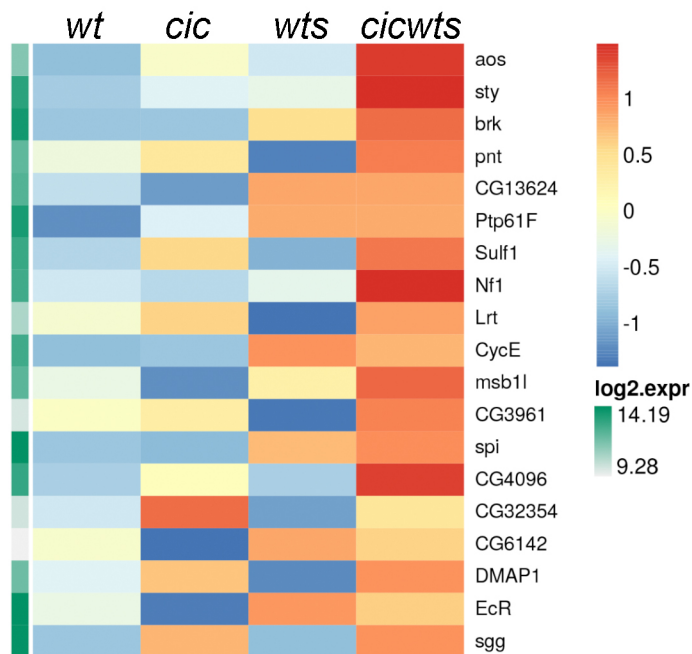
Suppl. Figure 1



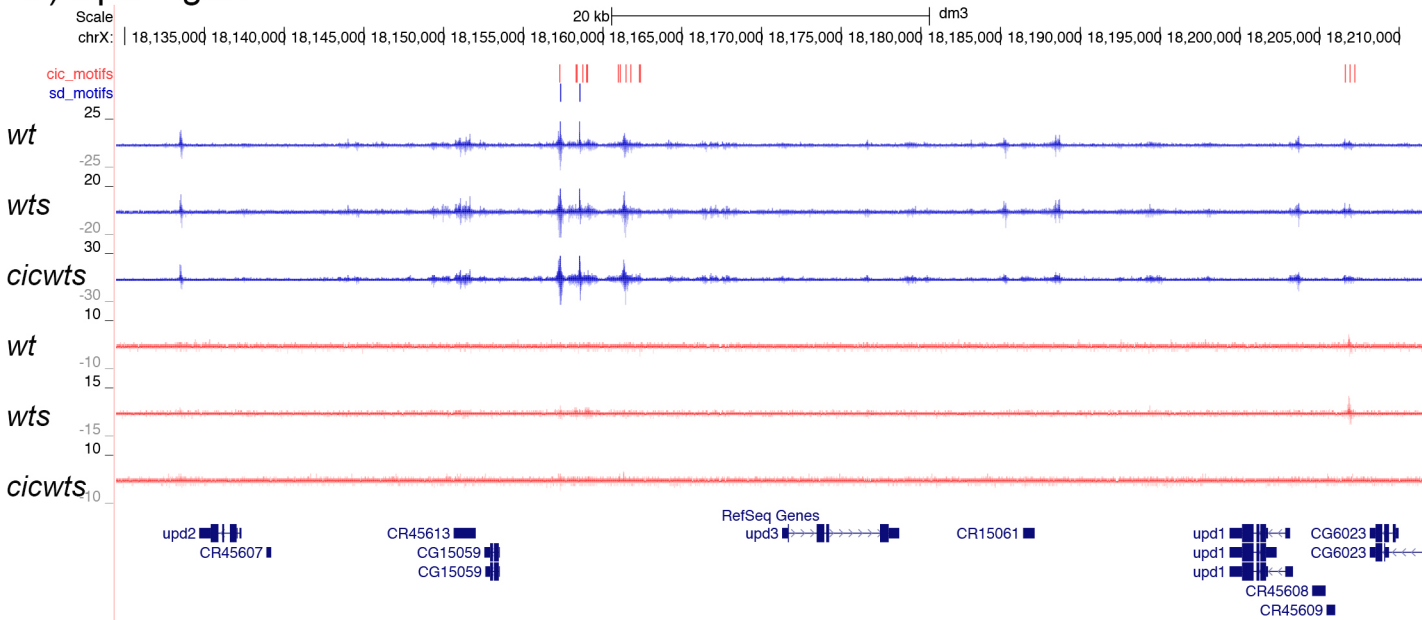
A) Synergistically induced genes



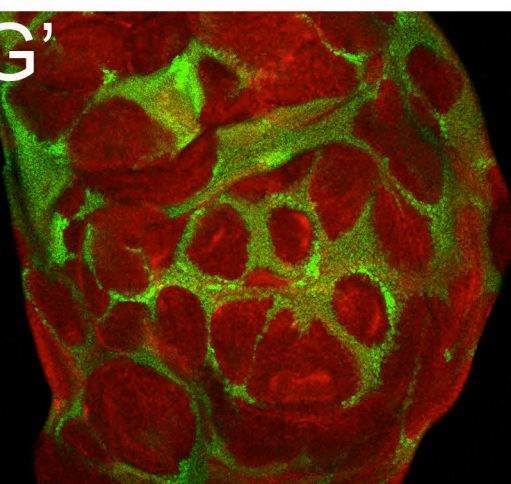
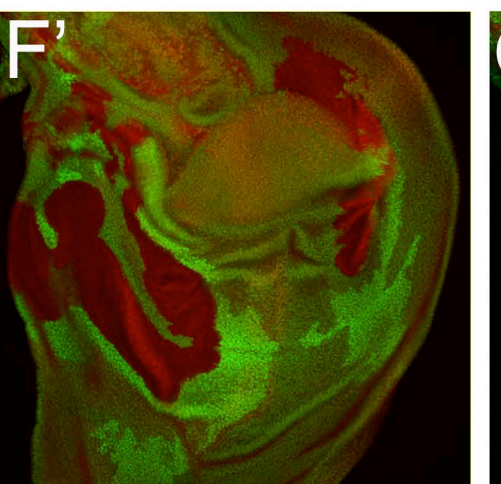
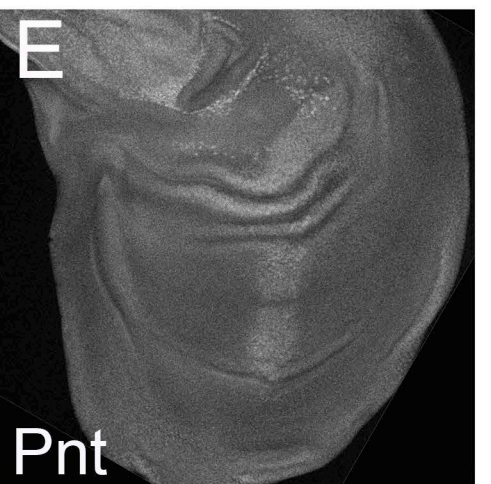
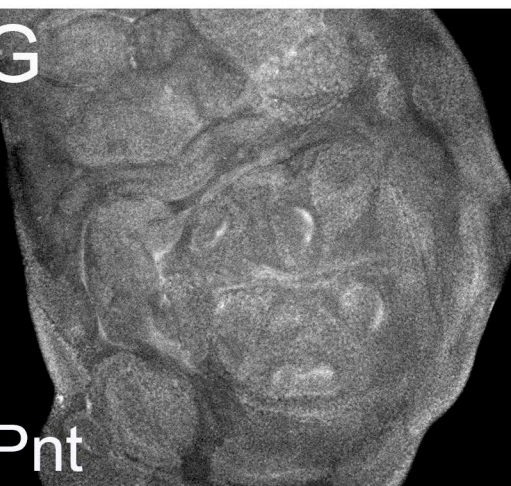
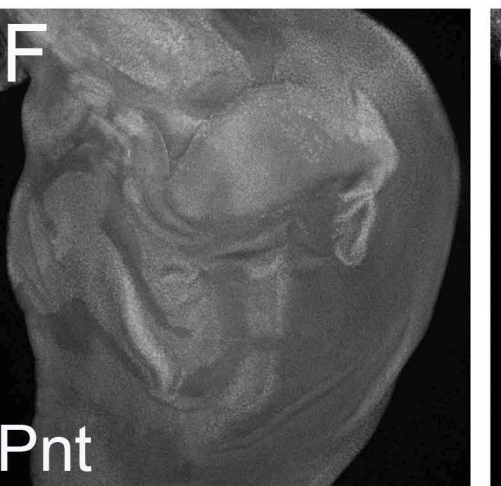
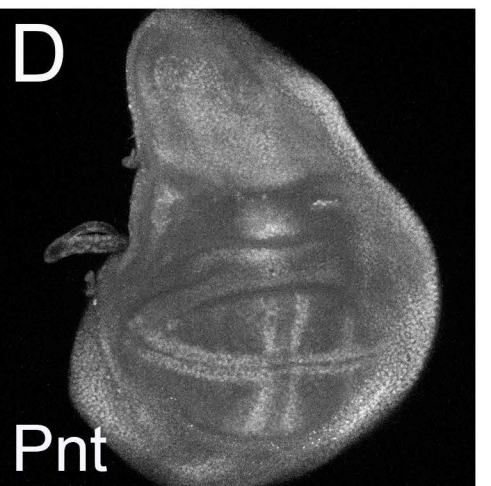
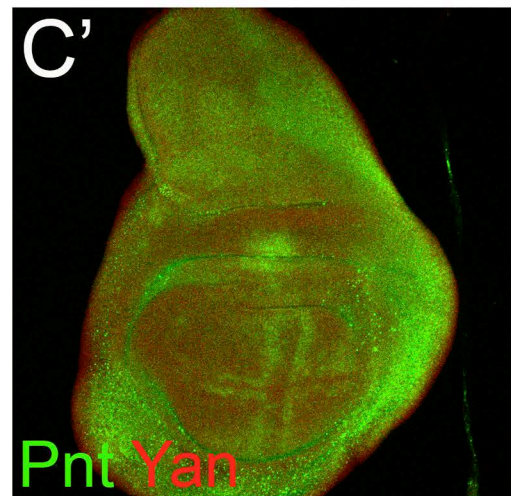
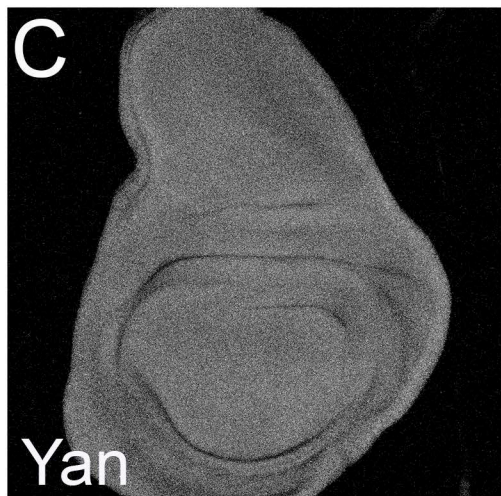
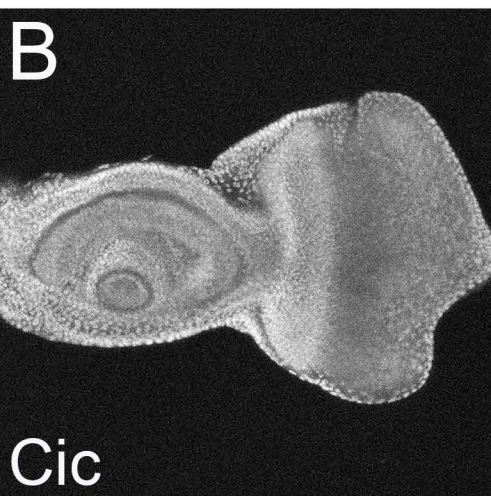
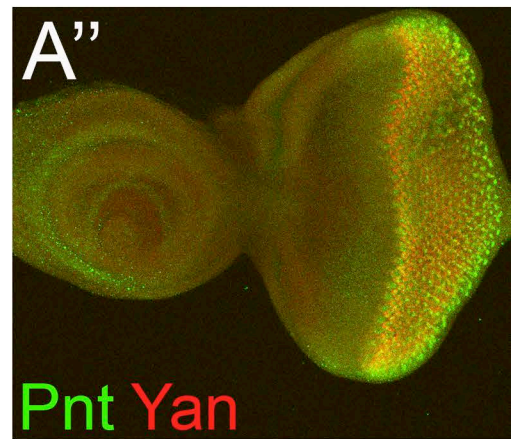
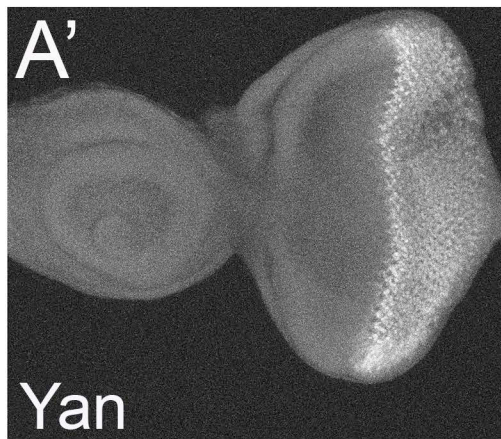
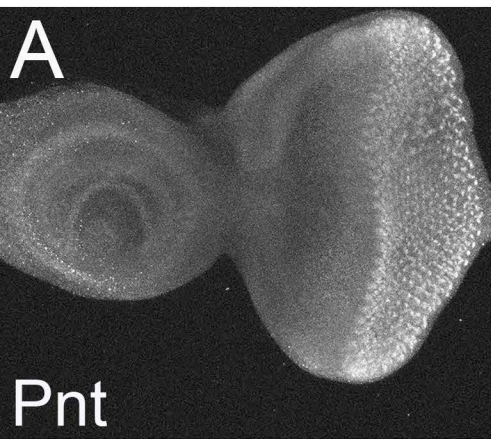
B) Direct Cic targets



C) Upd region



Suppl. Fig.3



ex

cic clones in ex

cic wts clones

